Determination of Sediment Provenance at Drift Sites Using Hydrogen Isotopes in Lipids

by

Amy C. Englebrecht

B.S. Geology
B.S. Environmental Science
Lake Superior State University, 2001

SUBMITTED TO THE DEPARTMENT OF EARTH, ATMOSPHERIC AND PLANETARY SCIENCES IN PARTIAL FULFILLMENT OF THE REQUIREMENTS FOR THE DEGREE OF

MASTER OF SCIENCE IN CHEMICAL OCEANOGRAPHY

at the

MASSACHUSETTS INSTITUTE OF TECHNOLOGY
and
WOODS HOLE OCEANOGRAPHIC INSTITUTION

FEBRUARY 2004

Signature of Author: ______________________
Department of Earth, Atmospheric and Planetary Sciences
January 15, 2004

Certified by: ______________________
Julian P. Sachs
Assistant Professor of Paleoclimatology
Thesis Supervisor

Accepted by: ______________________
Phil Gschwend
Chair, Joint Committee for Chemical Oceanography
Massachusetts Institute of Technology

Determination of sediment provenance at drift sites using hydrogen isotopes in lipids

Amy C. Englebrecht

Abstract--Paleoclimate records with sufficient length and temporal resolution to study the occurrence and causal mechanisms of abrupt climate change are exceedingly rare. Rapidly deposited ocean sediments provide the best archive for studying these events through geologic time, but such sites in the open ocean are limited to sediment drift deposits such as the Bermuda Rise in the northwest Atlantic. Using multiple climate proxies in a single core is becoming more common in high-resolution paleoclimate investigations, but a major potential concern for this approach arises from the possibility that the fine fraction of sediment (< 63 μm), and the climate proxies within it, may represent conditions far from the deposition site. We hypothesize that hydrogen isotope ratios of alkenones, a class of lipids from phytoplankton, may provide insight into the source of fine fraction sediment. Because of their restricted sources, broad geographic distribution, and excellent preservation properties, alkenones are of particular interest in the emerging field of compound-specific hydrogen isotopic analysis, and the sedimentary abundances, extents of unsaturations, and isotopic compositions of alkenones provide quantitative and near-continuous records. We isolated alkenones from cultured unicellular algae (haptophyte *Emiliania huxleyi*), surface ocean particulate material, and open ocean sediments to determine the extent and variability of hydrogen isotopic fractionation in the di-, tri-, and tetraunsaturated C_{37} compounds. We then compared the δD of the alkenones in surface sediments between the Bermuda Rise and the Scotian Margin above which a large (~20‰) δD gradient exists. We determined the fractionation between alkenones from suspended particulate samples and the water in which the phytoplanton lived, and examined the variability of alkenone δD during key climate transitions at the Bermuda Rise.

Thesis Supervisor: Julian P. Sachs

Table of Contents

List of Figures

List of Tables

Chapter 1: Introduction

1.1 Goals of Thesis

The goals of this thesis were to: 1) confirm predictability of $\Delta\delta D$ between environmental water and alkenones; 2) determine if initial D/H ratios of alkenones persist downcore in sediments; 3) use alkenone δD to elucidate origin of fine fraction sediment at the Bermuda Rise during key climate transitions.

1.2 Overview of Alkenones as a Paleoceanographic Proxy

Temporal records in cores from lakes and ocean sediments, in coral reefs, and in polar ice encode information on natural variations of the climate system. One of the most fundamental and important parameters needed to study ocean-climate linkages is sea surface temperature (SST). Geochemical proxies that reflect past environmental conditions are employed to understand large-scale shifts in climate, and in the mid-1980's a new paleo-SST proxy based on a class of sedimentary organic compounds called alkenones was introduced (Brassell et al., 1986b). This formed the basis for a new approach to paleoclimate study: molecular stratigraphy.

Emiliania huxleyi, a cosmopolitan coccolithophorid, is an abundant species in both open ocean and coastal waters and is noted for its propensity to form immense blooms that have a major impact on the biological carbon cycle and on atmosphere/ocean fluxes of carbon dioxide and volatile sulfur compounds (reviewed in Westbroek et al., 1993). *E. huxleyi* and *Gephyrocapsa oceanica*, a member of the genus from which *E. huxleyi* is believed to have evolved (Marlowe et al., 1990), are distinguished by their synthesis of a suite of C_{37}-C_{39} methyl and ethyl ketones, collectively called alkenones (Volkman et al., 1980; 1995; Figure 1). Although the location and biochemical function of these compounds within the cell is not presently known, it is recognized that the synthesis of alkenones is restricted taxonomically and has been documented only within the haptophyte order Isochrysidales (reviewed in Conte et al. 1994).

Alkenones gained attention after recognition that their degree of unsaturation is strongly controlled by the growth temperature of their producers (Marlowe, 1984) and that downcore

I Diunsaturated Compounds:

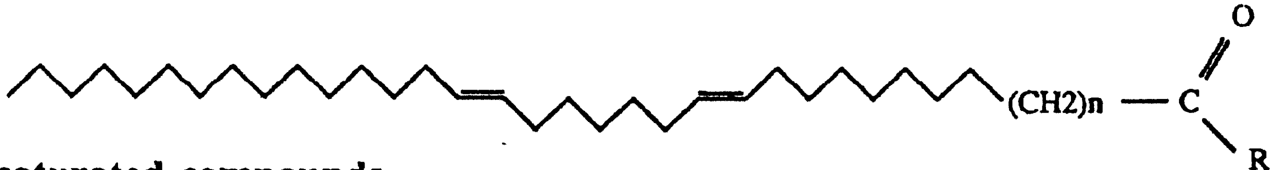

II Triunsaturated compounds

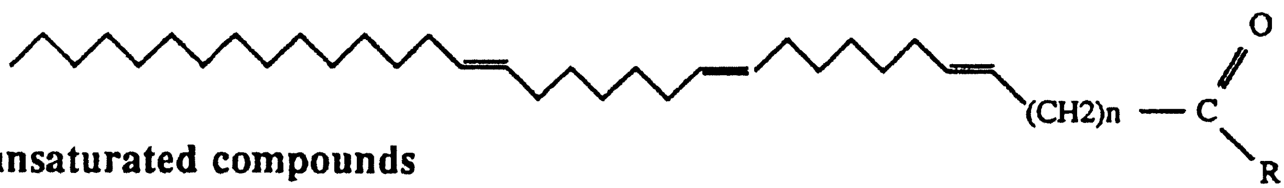

III Tetraunsaturated compounds

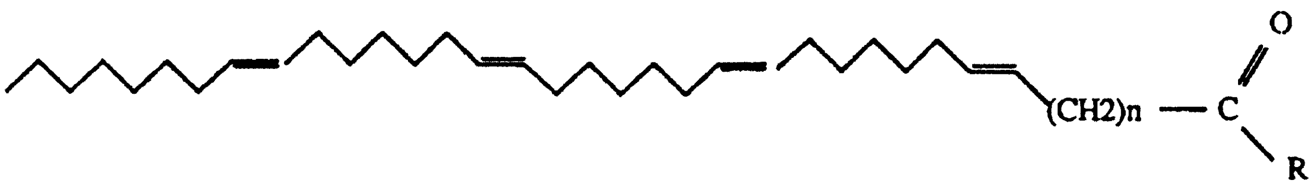

Figure 1.

(glacial-interglacial) variations in the ratio of di-, tri-, and tetraunsaturated alkenones closely corresponded with shifts in oxygen isotopic compositions of planktonic foraminifera (Brassell et al., 1986b). The unusual trans geometry of the double bonds (Rechka and Maxwell, 1988) may be responsible for preservation of the unsaturation ratios downcore, and alkenones have been demonstrated to be stable over time in the water column and during early diagenesis in sediments (Conte et al., 1992). Brassell et al. (1986a,b) defined an alkenone unsaturation index, [U^K_{37} = (37:2 - 37:4)/(37:2 + 37:3 + 37:4)] and proposed U^K_{37} could be used as an indicator of paleo-SST. Prahl et al. (1988) calibrated C_{37} alkenone unsaturation with growth temperature for a NE Pacific strain of *E. huxleyi*, and Prahl and Wakeham (1987) demonstrated that a modified index, $U^{K'}_{37}$ [= (37:2)/(37:2 + 37:3)] varied linearly with SST, with an accuracy in $U^{K'}_{37}$ value of ±0.02 units. This corresponds to a growth temperature precision of ±0.6°C (Prahl and Wakeham, 1987; Sikes and Volkman, 1993).

The sedimentary abundances, extents of unsaturations, and isotopic compositions of alkenones provide quantitative and near-continuous records, and along with restricted sources, broad geographic distribution, and excellent preservation properties, alkenones provide an opportunity to reconstruct paleo-SST on a global scale. These same characteristics make alkenones of particular interest in the emerging field of compound-specific hydrogen isotopic analysis.

1.3 Hydrogen Isotopes in the Environment

Stable hydrogen isotope ratios of modern and fossil organic substrates contain potentially valuable climatic information (Buchardt and Fritz, 1980; Yapp and Epstein, 1982; Smith et al., 1983; Schimmelmann et al., 1986; Miller et al., 1988; Friedman et al., 1988; Miller 1991). Trends in the distribution patterns of deuterium and oxygen-18 concentrations in meteoric waters (rain and snow) reveal a close correlation among some climatically relevant meteorological parameters, such as surface air temperature or amount and isotopic composition of precipitation (Craig, 1961; Dansgaard, 1964). Fractionation from non-equilibrium processes such as evaporation lead to imperfections in the correlation between $\delta^{18}O$ and δD, but the first order signals of $\delta^{18}O$ and δD can be used interchangeably (Dansgaard, 1964). That near-linear relationship is often plotted as the Global Meteoric Water Line (Figure 2). Using this

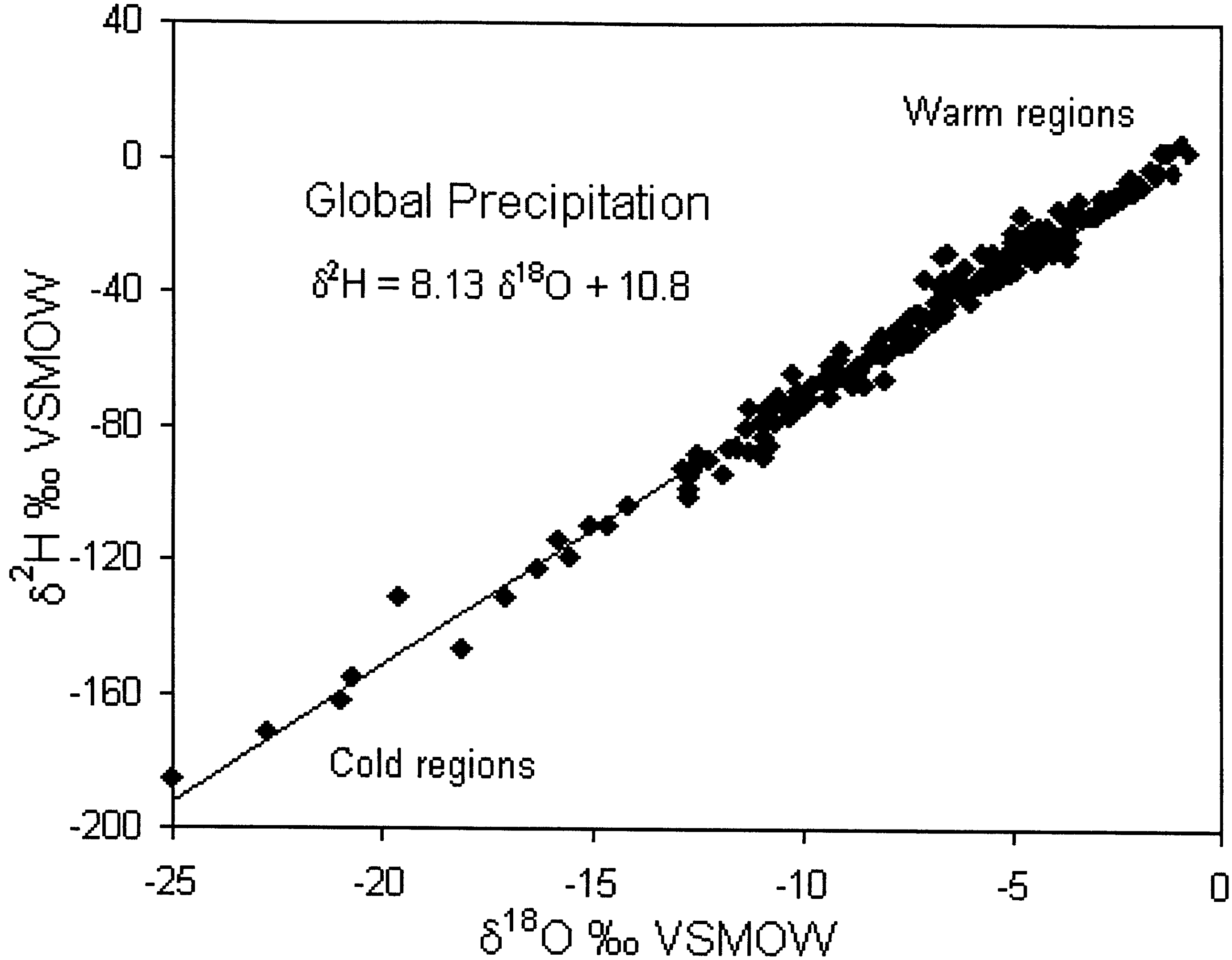

Warm regions
Global Precipitation
δ²H = 8.13 δ¹⁸O + 10.8
Cold regions
δ²H ‰ VSMOW
δ¹⁸O ‰ VSMOW
40
0
-40
-80
-120
-160
-200
-25
-20
-15
-10
-5
0

Figure 2.

relationship, [$\delta D \cong 8\delta^{18}O + 10$], and the extensive surface-ocean $\delta^{18}O$ data set available, a map of surface ocean δD has been constructed (Figure 3) and reveals a strong gradient in surface ocean δD in the northwest Atlantic. Analyses of water samples from this region confirming this gradient are presented in Chapter 2.

At low temperatures, water hydrogen exchanges quickly and reversibly with labile organic hydrogen, most of which is bound to organic nitrogen, sulfur, and oxygen (Koepp, 1978; Werstiuk and Ju, 1989), limiting the usefulness of measuring total D/H ratios in most organic compounds. Known exceptions are hydrocarbons and lipids (Schoell, 1984; Sternberg, 1988), nitrated cellulose (Epstein et al., 1976) and chemical derivatives of chitin (Schimmelmann and DeNiro, 1986; Miller et al., 1988). Water at neutral pH and low temperature in the absence of a catalyst does not readily exchange with most carbon-bound hydrogen, thereby conserving the D/H ratios of *n*-alkanes at temperatures well above 150°C (Koepp, 1978; Hoering, 1984). Only hydrogen in a few aromatic and alkyl sites adjacent to branching and carbonyl positions may start to reversibly exchange around 100°C (Alexander et al., 1981; Werstiuk and Ju, 1989), especially at low pH. In addition to these reversible processes, irreversible hydrogen isotopic exchange may occur as a consequence of chemical reactions of organic matter. Sufficient activation energies to break carbon bonds, such as that provided by exposure to radiation (Dahl et al., 1988) or high temperatures (Hoering, 1984; Seewald et al., 1998), as well as reactions involving radicals (Schoell, 1984) facilitate isotopic exchange between C-H and ambient water hydrogen.

1.4 Hydrogen Isotopes in Lipids

Hydrogen isotopic compositions of lipids are controlled by three factors: isotopic compositions of biosynthetic precursors, fractionation and exchange accompanying biosynthesis (Martin et al., 1986), and hydrogenation during biosynthesis (Smith and Epstein, 1970; Luo et al., 1991). Sternberg (1988) examined lipids in submerged aquatic plants and found hydrogen isotopes fractionate predictably, thereby recording the D/H ratio of environmental water. Sessions and coworkers (1999) developed a reliable analytical system capable of measuring the D/H ratio of individual organic compounds, leading to the discovery that while different compounds within a given class (e.g. sterols) can have substantially different δD in different

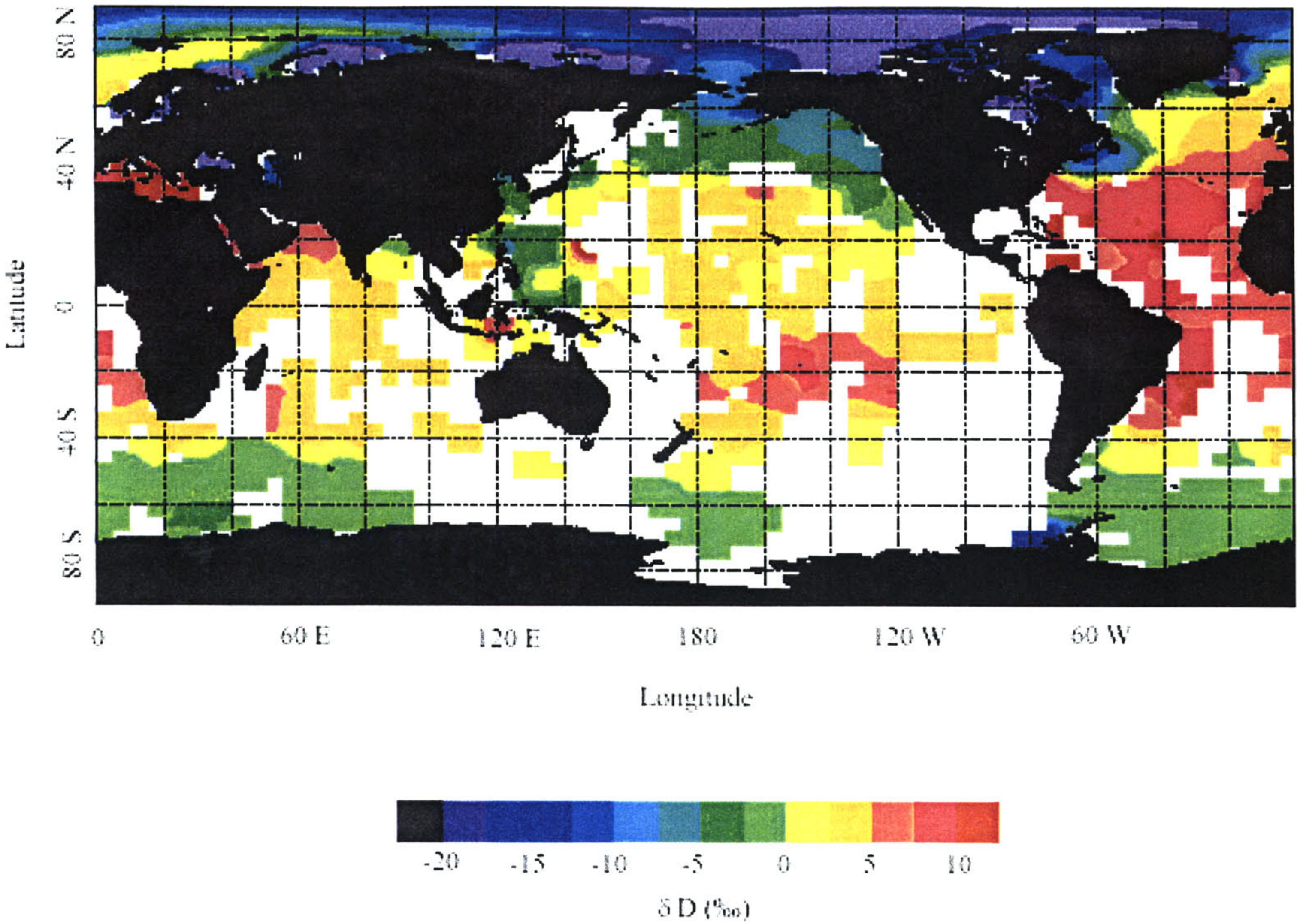
80 N
40 N
0
40 S
80 S
Latitude
0
60 E
120 E
180
120 W
60 W
Longitude
-20
-15
-10
-5
0
5
10
δ D (‰)

Figure 3.

organisms despite growing in water with the same hydrogen isotopic composition, there was little isotopic variability within specific compound classes in individual organisms, and δD of individual lipids in each class generally fell within a range of < 50‰ (Sessions et al., 1999).

1.5 Studying Paleoclimate at the Bermuda Rise

Paleoclimate records with sufficient length and temporal resolution to study the occurrence and causal mechanisms of abrupt climate change are exceedingly rare. Rapidly deposited ocean sediments provide the best archive for studying these events through geologic time, but such sites in the open ocean are limited to sediment-drift deposits such as the Bermuda Rise in the northwest Atlantic Ocean (Figure 4). In the deep ocean away from continental margins, sediments consist entirely of material from the upper ocean that is a mixture of sand-sized (>63 μm) particles, mostly of foraminiferal origin, and fine particles (<63 μm) that consist of wind-blown dust and phytoplankton detritus. But sedimentation rates at open ocean sites are extremely low, on the order of a few centimeters per 1000 years, or in the case of the North Pacific, less than one centimeter per 1000 years. In drift deposits, however, flux of laterally transported sediment exceeds vertical flux, leading to high accumulation rates (Bacon and Rosholt, 1982; Bacon, 1984; Suman and Bacon, 1989), sometimes up to 1-2 m of sediment per 1000 years.

Using geochemical (e.g. Sachs and Lehman, 1999; Sachs et al., 2001), faunal (e.g. McManus et al., 1994; Keigwin and Pickart, 1999; Lehman et al., 2002), and isotopic (e.g. Keigwin and Jones, 1989; Charles et al., 1996; Keigwin, 1996; Adkins et al., 1997; Raymo et al., 1998; Draut et al., 2003) proxies, many studies have targeted drift sites to construct detailed paleoclimate records and improve understanding of abrupt climate change. To avoid mistaken interpretations, it is important to develop parallel, independent proxy records that can provide constraints and confirmations. The use of multiple climate proxies in a single core is becoming more common in high-resolution paleoclimate investigations and, in this approach, the assumption is made that climate proxies measured in the same depth interval of sediment represent the same interval of time. This circumvents chronological uncertainties associated with comparing proxy records from different cores whose age models have substantial uncertainties. In addition, multiple proxies of the same physical parameter, such as SST, can be

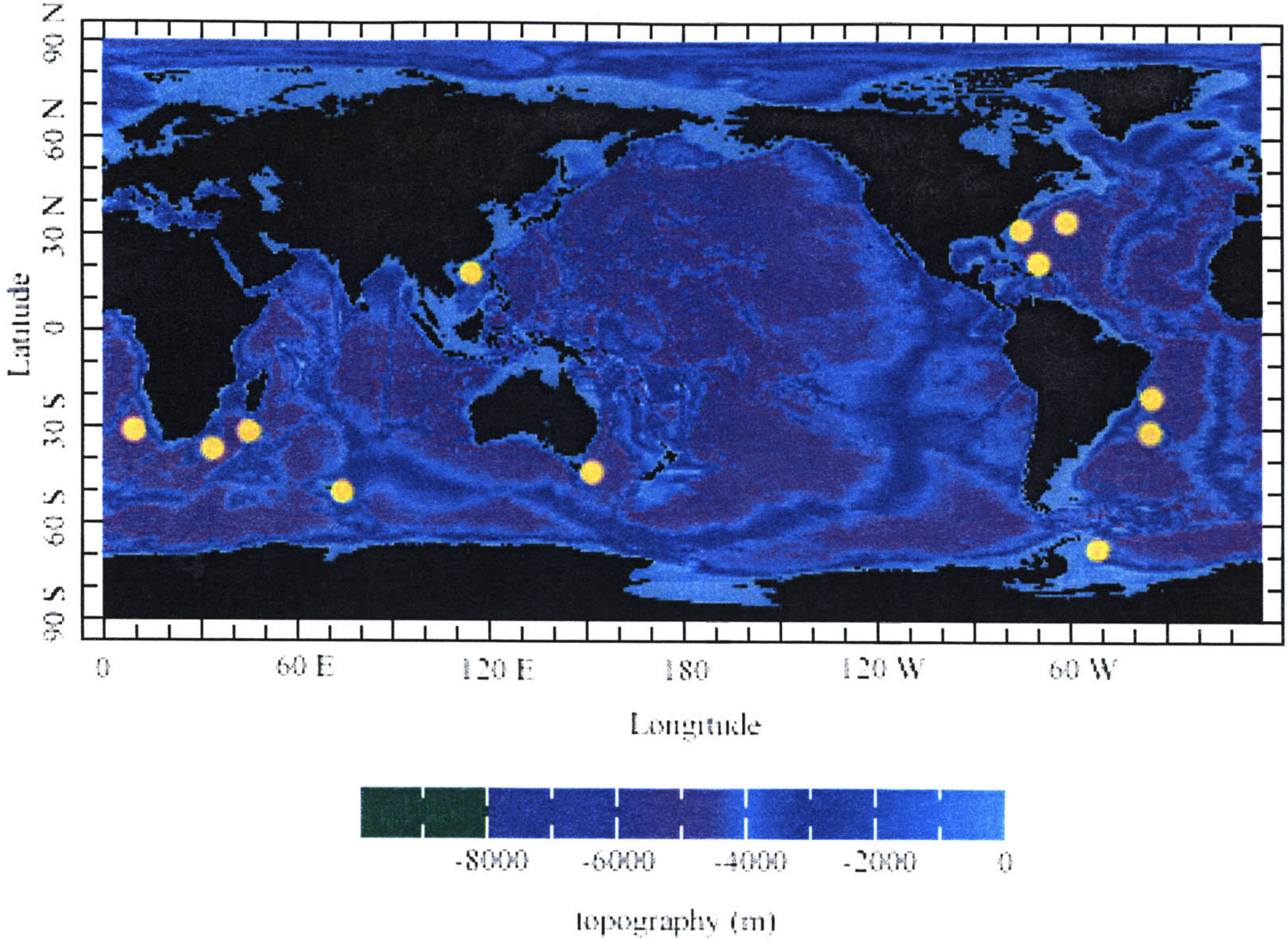
90 N
60 N
30 N
0
30 S
60 S
90 S
Latitude
0
60 E
120 E
180
120 W
60 W
Longitude
-8000
-6000
-4000
-2000
0
topography (m)

Figure 4.

measured in a single core to determine how depth and seasonality may have contributed to the "temperature history" recorded by different proxies whose measurement in isolation would have been interpreted as *the* temperature history.

Because lateral transport predominates over vertical sedimentation at drift deposits, careful consideration must be given to the role horizontal advection of sediment may play in shaping downcore records of proxies that are part of the fine fraction of sediment. A major potential concern for utilizing the multiple proxy approach at drift sites arises from the possibility that the climate proxies associated with the fine fraction of sediment (e.g., alkenone unsaturation ratios, clay mineralogy, detrital Sr and Nd isotopic ratios) may be chronologically and spatially decoupled from those associated with the coarse fraction of sediment (e.g., abundance, isotope ratio, and trace metal concentration of foraminiferal tests; Ohkouchi et al., 2002). The recognition and determination of the magnitude of offsets between proxies is particularly important when records of abrupt climate change are sought from these types of high deposition rate sites. On the Bermuda Rise, for example, high rates of sedimentation are maintained by lateral advection and focusing of distal fine-grained sediments that are believed to derive predominantly from the Canadian margin off Nova Scotia (Laine and Hollister, 1981; Keigwin and Jones, 1989; Suman and Bacon, 1989; Figure 5). Ohkouchi and coworkers (2002) demonstrated that at the same level in a Bermuda Rise sediment core, the radiocarbon ages of alkenones greatly exceed those of foraminifera, and concluded that in the strata studied, some aspects of the fine material cannot be interpreted as a time history of events at the sea surface directly above the site.

1.6 Organization of Thesis

Procedures for the isolation of alkenones and analysis of their hydrogen isotopic ratios are presented in Section 2.3. Results from culturing experiments confirming the predictability of the expression of environmental D/H ratios in the δD of lipids are presented in Section 3.2.1 and results from a suite of marine particulate and sediment samples are presented in Section 3.2.2. Finally, in Section 3.2.3, we present evidence that alkenone δD analyses are a complementary approach to the alkenone ^{14}C age determination pioneered by Ohkouchi et al. (2002) because while ^{14}C work can indicate the variability of the processes affecting the fine fraction signal, the

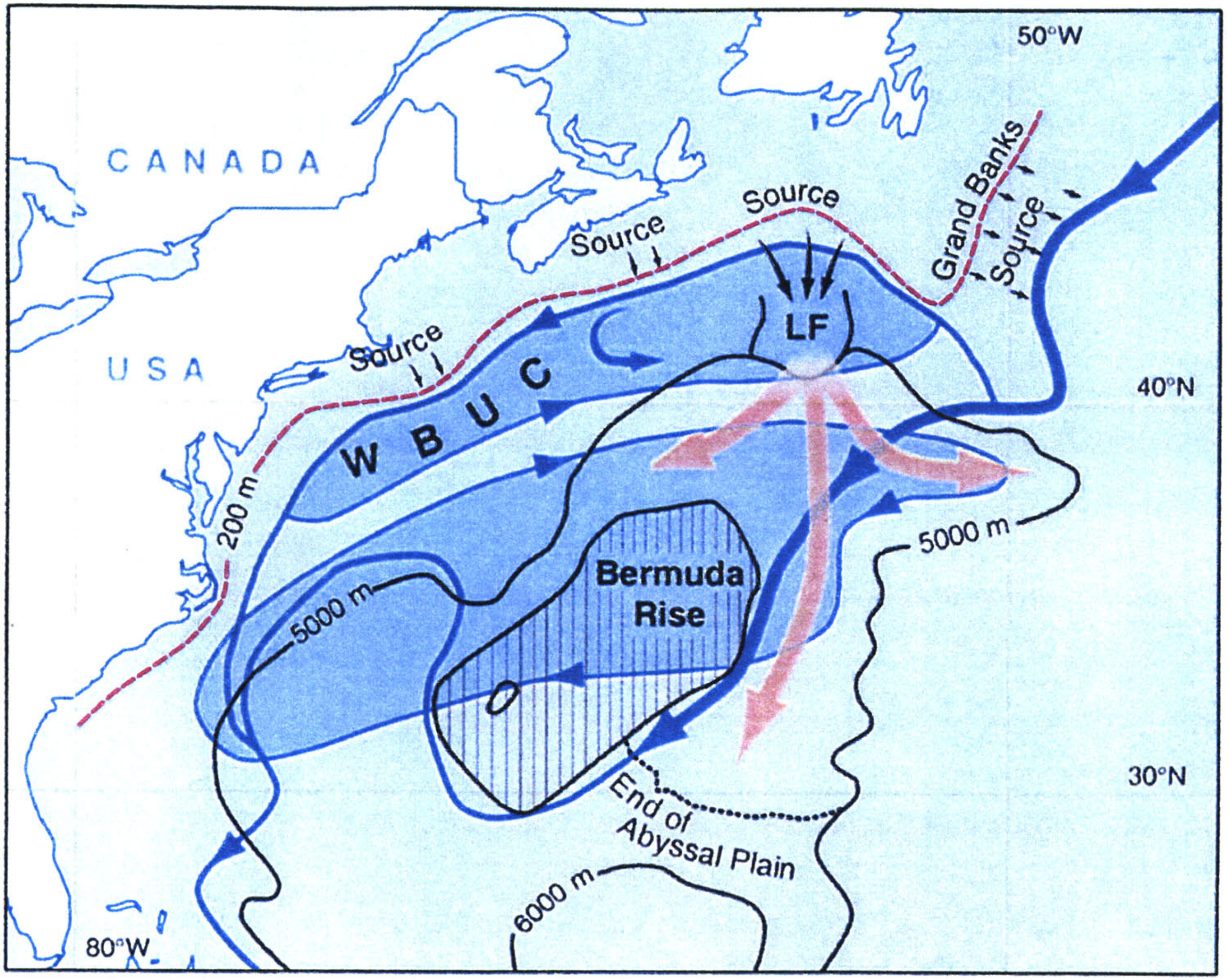

50°W
CANADA
USA
Source
Source
Source
Grand Banks
Source
LF
WBUC
40°N
200 m
5000 m
Bermuda
Rise
5000 m
30°N
End of
Abyssal Plain
6000 m
80°W

Figure 5.

alkenone δD signature allows analysis of the regions from which the fine material is derived. Further, the alkenone hydrogen isotopic evidence suggests the source of the fine fraction of sediment at the Bermuda Rise has shifted during the last 1300 yr BP.

References for Chapter 1

Adkins J. F., Boyle E. A., Keigwin L., and Cortijo E. (1997) Variability of the North Atlantic thermohaline circulation during the last interglacial period. *Nature* **390,** 154-156.

Alexander R., Kagi R. I., Larcher A. V. and Woodhouse G. W. (1981) Aromatic hydrogen exchange in petroleum source rocks. In *Advances in Organic Geochemistry, 1981* (ed. M. Bjoroy et al.) pp. 69-71. Wiley.

Bacon M. P. (1984) Glacial to interglacial changes in carbonate and clay sedimentation in the Atlantic Ocean estimated from ^{230}Th measurements. *Isotope Geosci.* **2,** 97-111.

Bacon M. P. and Rosholt J. N. (1982) Accumulation rates of Th-230, Pa-231, and some transition metals on the Bermuda Rise. *Geochim. Cosmochim. Acta* **46,** 651-666.

Brassell S. C., et al. (1986a) Palaeoclimatic signals recognized by chemometric treatment of molecular stratigraphic data. *Org. Geochem.* **10,** 661-669.

Brassell S. C., Eglinton G., Marlowe I. T., Pflaumann U. and Sarnthein M. (1986b) Molecular stratigraphy: a new tool for climatic assessment. *Nature* **320,** 129-133.

Buchardt B. and Fritz P. (1980) Environmental isotopes as environmental and climatological indicators. In *Handbook of Environmental Isotope Geochemistry,* Vol. 1 (ed. P. Fritz and J. C. Fontes) pp. 473-504. Elsevier, Amsterdam.

Charles C. D., Lynch-Stieglitz J., Ninnemann U. S. and Fairbanks R. G. (1996) Climate connections between the hemispheres revealed by deep sea sediment core / ice core correlations. *Earth Planet. Sci. Lett.* **142,** 19-27.

Conte M. H., Eglinton G. and Madureira L. A. S. (1992) Long-chain alkenones and alkyl alkenoates as paleotemperature indicators: their production, flux and early sedimentary diagenesis in the Eastern North Atlantic. *Org. Geochem.* **19,** 287-298.

Conte M. H., Thompson A., Lesley D. and Harris R. P. (1998) Genetic and physiological influences on the alkenone/alkenoate versus growth temperature relationship in *Emiliania huxleyi* and *Gephyrocapsa oceanica. Geochim. Cosmochim. Acta* **62,** 51-68.

Conte M. H., Volkman J. K. and Eglinton G. (1994) Lipid biomarkers of the Haptophyta. In *The Haptophyte Algae* (ed. J. C. Green and B. S. C. Leadbeater) pp. 351-77. Clarendon Press.

Craig H. (1961) Isotopic variations in meteoric waters. *Science* **133,** 1702-1703.

Dahl J., Hallberg R. and Kaplan I. R. (1988) The effects of radioactive decay of uranium on elemental and isotopic ratios of Alum Shale kerogen. *Appl. Geochem.* **3,** 583-589.

Dansgaard W. (1964) Stable isotopes in precipitation. *Tellus* **16,** 436-468.

Draut A. E., Raymo M. E., McManus J. F. and Oppo D. W. (2003) Climate stability during the Pliocene warm period. *Paleoceanography* **18,** 1078-1089.

Epstein S., Yapp C. J. and Hall J. H. (1976) The determination of the D/H ratios of non-exchangeable hydrogen in cellulose extracted from aquatic and land plants. *Earth and Planet. Sci. Lett.* **30,** 241-251.

Friedman I., Carrara P. and Gleason J. (1988) Isotopic evidence of Holocene climatic change in the San Juan Mountains, Colorado. *Quat. Res.* **30,** 350-353.

Hoering T. C. (1984) Thermal reactions of kerogen with added water, heavy water, and pure organic substances. *Org. Geochem.* **5,** 267-278.

Keigwin L. D. (1996) The Little Ice Age and Medieval Warm Period in the Sargasso Sea. *Science* **274,** 1504-1508.

Keigwin L. D. and Jones G. A. (1989) Glacial-Holocene stratigraphy, chronology, and paleoceanographic observations on some North Atlantic sediment drifts. *Deep-Sea Res.* **36,** 845-867.

Keigwin L. D. and Pickart R. S. (1999) Slope water current over the Laurentian Fan on interannual to millennial time scales. *Science* **286,** 520-523.

Koepp M. (1978) D/H isotope exchange reaction between petroleum and water: a contributory determinant for D/H-isotope ratios in crude oils? In *Short papers of the 4th International Conference, Geochronology, Cosmochronology, Isotope Geology. USGS Open File Report* (ed. R.E. Zartman) pp. 78-701. US Geological Survey.

Laine E. P. and Hollister C. D. (1981) Geological effects of the Gulf Stream system on the Northern Bermuda Rise. *Mar. Geol.* **39,** 277-310.

Lehman S. J., Sachs J. P., Crotwell A. M., Keigwin L. D. and Boyle E. A. (2002) Relation of subtropical Atlantic temperature, high-latitude ice rafting, deep water formation, and European climate 130,000-60,000 years ago. *Quat. Sci. Rev.* **21,** 1917-1924.

Luo Y-H., Sternberg L. dS. L., Suda S., Kumazawa S. and Mitsui A. (1991) Extremely low D/H ratios of photoproduced hydrogen by cyanobacteria. *Plant Cell Phys.* **32,** 897-900.

Marlowe I. T. (1984) Lipids as paleoclimatic indicators. Ph.D. Dissertation, Univ. Bristol.

Marlowe I. T., Brassell S. C., Eglinton G. and Green J.C. (1990) Long-chain alkenones and alkyl alkenoates and the fossil coccolith record of marine sediments. *Chem. Geol.* **88,** 349-375.

Martin G. J., Zhang B. L., Naulet N. and Martin M. L. (1986) Deuterium transfer in the bioconversion of glucose to ethanol studied by specific isotope labeling at the natural abundance level. *J. Amer. Chem. Soc.* **108,** 5116-5122.

McCave I. N. (2002) A Poisoned Chalice? *Science* **298,** 1186-1187.

McManus J. F., Bond G. C., Broecker W. S., Johnsen S., Labeyrie L. and Higgins S. (1994) High-resolution climate records from the North Atlantic during the last interglacial. *Nature* **371,** 326-329.

Miller R. F. (1991) Chitin paleoecology. *Biochem. Sys. Ecol.* **19,** 401-411.

Miller R. F., Fritz P. and Morgan A. V. (1988) Climatic implications of D/H ratios in beetle chitin. *Palaeogeog. Palaeoclim. Palaeoecol.* **66,** 277-288.

Ohkouchi N., Eglinton T. I., Keigwin L. D. and Hayes J. M. (2002). Spatial and temporal offsets between proxy records in a sediment drift. *Science* **298,** 1224-1227.

Prahl F. G., Meuhlhausen L. A. and Zahnle D. L. (1988) Further evaluation of long-chain alkenones as indicators of paleoceanographic conditions. *Geochim. Cosmochim. Acta* **52,** 2303-2310.

Prahl F. G. and Wakeham S. G. (1987) Calibration of unsaturation patterns in long-chain ketone compositions for palaeotemperature assessment. *Nature* **330,** 367-369.

Raymo M. E., Ganley K., Carter S., Oppo D. W. and McManus J. (1998) Millennial-scale climate instability during the early Pleistocene epoch. *Nature* **392,** 699-702.

Rechka J. A. and Maxwell J.R. (1988) Characterization of alkenone temperature indicators in sediments and organisms. *Org. Geochem.* **13,** 727-734.

Rozanski K., Araguas-Araguas L. and Gonfiantini R. (1992) Relation between long-term trends of oxygen-18 isotope composition of precipitation and climate. *Science* **258,** 981-985.

Sachs J. P., Anderson R. F. and Lehman S. J. (2001) Glacial surface temperatures of the Southeast Atlantic Ocean. *Science* **293,** 2077-2079.

Sachs J. P. and Lehman S. J. (1999) Subtropical North Atlantic temperatures 60,000 to 30,000 years ago. *Science* **286,** 756-759.

Sauer P. E., Eglinton T. I., Hayes J. M., Schimmelmann A. and Sessions A. L. (2001) Compound-specific D/H rations of lipid biomarkers from sediments as a proxy for environmental and climatic conditions. *Geochim. Cosmochim. Acta* **65,** 213-222.

Schimmelmann A. and DeNiro M. J. (1986) Stable isotopic studies on chitin III. The $^{18}O/^{16}O$ and D/H ratios in arthropod chitin. *Geochim. Cosmochim. Acta* **50,** 1485-1496.

Schimmelmann A., DeNiro M. J., Poulicek M., Voss-Foucart M.-F., Goffinet G. and Jeauniaux C. (1986) Isotopic composition of chitin from arthropods recovered in archaeological contexts as palaeoenvironmental indicators. *J. Archaeol. Sci.* **13,** 553-566.

Schmidt G. A., Bigg G. R. and Rohling E. J. (1999) Global seawater oxygen-18 database. http://www.giss.nasa.gov/data/o18data/

Schoell M. (1984) Stable isotopes in petroleum research. *Adv. Petrol. Geochem.* **1,** 215-245.

Seewald J. S., Benitez-Nelson B. C. and Whelan J. K. (1998) Laboratory and theoretical constraints on the generation and composition of natural gas. *Geochim. Cosmochim. Acta* **62,** 1599-1617.

Sessions A. L., Burgoyne T. W., Shimmelmann A. and Hayes J. M. (1999) Fractionation of hydrogen isotopes in lipid biosynthesis. *Org. Geochem.* **30,** 1193-2000.

Sikes E. L. and Volkman J. K. (1993) Calibration of alkenone unsaturation ratios ($U^{K'}_{37}$) for paleotemperature estimation in cold polar waters. *Geochim. Cosmochim. Acta* **57,** 1883-1889.

Smith J. W., Rigby D., Schmidt P. W. and Clark D. A. (1983) D/H ratios of coals and the paleoaltitude of their deposition. *Nature* **302,** 322-323.

Smith B. N. and Epstein S. (1970) Biogeochemistry of the stable isotopes of hydrogen and carbon in salt marsh biota. *Plant Phys.* **46,** 738-742.

Sternberg L. dS. L. (1988) D/H ratios of environmental water recorded by D/H ratios of plant lipids. *Nature* **333,** 59-61.

Suman D. O. and Bacon M. P. (1989) Variations in Holocene sedimentation in the North American Basin determined from ^{230}Th measurements. *Deep Sea Res.* **36,** 869-878.

Volkman J. K., Barrett S. M., Blackburn S. I. and Sikes E. L. (1995) Alkenones in *Gephyrocapsa oceanica*: implications for studies of paleoclimate. *Geochim. Cosmochim. Acta* **59,** 513-520.

Volkman J. K., Eglinton G., Corner E. D. S. and Sargent J. R. (1980) Novel unsaturated straight-chain methyl and ethyl ketones in marine sediments and a coccolithophore *Emiliania huxleyi*. In *Advances in Organic Geochemistry, 1979* (ed. A. G. Douglas and J. R. Maxwell) pp. 219-227. Pergamon, Tarrytown, N.Y.

Werstiuk N. H. and Ju C. (1989) Protium-deuterium exchange of benzo-substituted heterocycles in neutral D_2O at elevated temperatures. *Can. J. Chem.* **67,** 812-815.

Westbroek P., et al. (1993) A model system approach to biological climate forcing: the example of *Emiliania huxleyi*. *Global Planet. Change* **8,** 27-46.

Yapp C. J. and Epstein S. (1982) Climatic significance of the hydrogen isotope ratios in tree cellulose. *Nature* **297,** 636-639.

Chapter 2

Determination of sediment provenance at drift sites using hydrogen isotopes in lipids

Amy C. Englebrecht and Julian Sachs

For submission to 'Geochimica et Cosmochimica Acta'

Abstract--Paleoclimate records with sufficient length and temporal resolution to study the occurrence and causal mechanisms of abrupt climate change are exceedingly rare. Rapidly deposited ocean sediments provide the best archive for studying these events through geologic time, but such sites in the open ocean are limited to sediment drift deposits such as the Bermuda Rise in the northwest Atlantic. Using multiple climate proxies in a single core is becoming more common in high-resolution paleoclimate investigations, but a major potential concern for this approach arises from the possibility that the fine fraction of sediment (< 63 μm), and the climate proxies within it, may represent conditions far from the deposition site. We hypothesize that hydrogen isotope ratios of alkenones, a class of lipids from phytoplankton, may provide insight into the source of fine fraction sediment. Because of their restricted sources, broad geographic distribution, and excellent preservation properties, alkenones are of particular interest in the emerging field of compound-specific hydrogen isotopic analysis, and the sedimentary abundances, extents of unsaturations, and isotopic compositions of alkenones provide quantitative and near-continuous records. We isolated alkenones from cultured unicellular algae (haptophyte *Emiliania huxleyi*), surface ocean particulate material, and open ocean sediments to determine the extent and variability of hydrogen isotopic fractionation in the di-, tri-, and tetraunsaturated C_{37} compounds. We then compared the δD of the alkenones in surface sediments between the Bermuda Rise and the Scotian Margin above which a large (~20‰) δD gradient exists. We determined the fractionation between alkenones from suspended particulate samples and the water in which the phytoplanton lived, and examined the variability of alkenone δD during key climate transitions at the Bermuda Rise.

1. INTRODUCTION

Emiliania huxleyi, a cosmopolitan coccolithophorid, is an abundant species in both open ocean and coastal waters and are distinguished by their synthesis of a suite of C_{37}-C_{39} methyl and ethyl ketones, collectively called alkenones (Volkman et al., 1980; 1995; Figure 1). Although the location and biochemical function of these compounds within the cell is not presently known, it is recognized that the synthesis of alkenones is restricted taxonomically and has been documented only within the haptophyte order Isochrysidales (reviewed in Conte et al. 1994).

Stable hydrogen isotope ratios of modern and fossil organic substrates contain potentially valuable climatic information (Buchardt and Fritz, 1980; Yapp and Epstein, 1982; Smith et al., 1983; Schimmelmann et al., 1986; Miller et al., 1988; Friedman et al., 1988; Miller 1991). Trends in the distribution patterns of deuterium and oxygen-18 concentrations in meteoric waters (rain and snow) reveal a close correlation (Craig, 1961; Dansgaard, 1964). Fractionation from non-equilibrium processes such as evaporation lead to imperfections in the correlation between $\delta^{18}O$ and δD, but the first order signals of $\delta^{18}O$ and δD may be used interchangeably (Dansgaard, 1964). Using the relationship, [$\delta D \cong 8\delta^{18}O + 10$], and the extensive surface ocean $\delta^{18}O$ data set available, a map of surface ocean δD has been constructed (Figure 3) and reveals a strong gradient in surface ocean δD in the northwest Atlantic.

At low temperatures, water hydrogen exchanges quickly and reversibly with labile organic hydrogen, most of which is bound to organic nitrogen, sulfur, and oxygen (Koepp, 1978; Werstiuk and Ju, 1989), limiting the usefulness of measuring total D/H ratios in most organic compounds. Known exceptions are hydrocarbons and lipids (Schoell, 1984; Sternberg, 1988), nitrated cellulose (Epstein et al., 1976) and chemical derivatives of chitin (Schimmelmann and DeNiro, 1986; Miller et al., 1988). Water at neutral pH and low temperature in the absence of a catalyst does not readily exchange with most carbon-bound hydrogen, thereby conserving the D/H ratios of *n*-alkanes at temperatures well above 150°C (Koepp, 1978; Hoering, 1984).

Hydrogen isotopic compositions of lipids are controlled by three factors: isotopic compositions of biosynthetic precursors, fractionation and exchange accompanying biosynthesis (Martin et al., 1986), and hydrogenation during biosynthesis (Smith and Epstein, 1970; Luo et al., 1991). Sternberg (1988) examined lipids in submerged aquatic plants and found hydrogen isotopes fractionate at a predictable rate, thereby recording the D/H ratio of environmental water.

Sessions and coworkers (1999) developed a reliable analytical system capable of measuring the D/H ratio of individual organic compounds, leading to the discovery that while different compounds within a given class (e.g. sterols) can have substantially different δD in different organisms despite growing in water with the same hydrogen isotopic composition, there was little isotopic variability within specific compound classes in individual organisms, and δD of individual lipids in each class generally fell within a range of < 50‰, (Sessions et al., 1999).

Using geochemical (e.g. Sachs and Lehman, 1999; Sachs et al., 2001), faunal (e.g. McManus et al., 1994; Keigwin and Pickart, 1999; Lehman et al., 2002), and isotopic (e.g. Keigwin and Jones, 1989; Charles et al, 1996; Keigwin, 1996; Adkins et al., 1997; Raymo et al., 1998; Draut et al., 2003) proxies, many studies have targeted drift sites to construct detailed paleoclimate records and improve understanding of abrupt climate change. To avoid mistaken interpretations, it is important to develop parallel, independent proxy records that can provide constraints and confirmations. In addition, multiple proxies of the same physical parameter, such as SST, can be measured in a single core to determine how depth and seasonality may have contributed to the "temperature history" recorded by different proxies whose measurement in isolation would have been interpreted as *the* temperature history. The use of multiple climate proxies in a single core is becoming more common in high-resolution paleoclimate investigations, and in this approach, the assumption is made that climate proxies measured in the same depth interval of sediment represent the same interval of time. This circumvents chronological uncertainties associated with comparing proxy records from different cores whose age models have substantial uncertainties.

Because lateral transport predominates over vertical sedimentation at drift deposits, careful consideration must be given to the role horizontal advection of sediment may play in shaping down-core records of proxies that are part of the fine fraction of sediment. A major potential concern for utilizing the multiple proxy approach at drift sites arises from the possibility that the climate proxies associated with the fine fraction of sediment (e.g., alkenone unsaturation ratios, biomarkers, clay mineralogy, detrital Sr and Nd isotopic ratios) may be chronologically and spatially decoupled from those associated with the coarse fraction of sediment (e.g., abundance, isotope ratio, and trace metal concentration of foraminiferal tests; Ohkouchi et al., 2002). The recognition and determination of the magnitude of offsets between proxies is particularly important when records of abrupt climate change are sought from high accumulation-rate sites. On the Bermuda Rise, for example, high rates of sedimentation are maintained by lateral advection and focusing of distal fine-grained sediments that are believed to derive predominantly from the Canadian margin off Nova Scotia (Laine and Hollister, 1981; Keigwin and Jones, 1989; Suman and Bacon, 1989; Figure 5). Ohkouchi and coworkers (2002) demonstrated that at the same level in a Bermuda Rise sediment core, the radiocarbon ages of alkenones greatly exceed those of foraminifera, and concluded that in the strata studied, some aspects of the fine material cannot be interpreted as a time history of events at the sea surface directly above the site.

The purposes of this study were to: 1) determine the fidelity by which alkenone δD reflects water δD in which coccolithophorids grow, both in culture and in the field; 2) determine if D/H ratios of sedimentary alkenones reflect the δD of suspended particles in surface waters over the site; and 3) apply alkenone δD measurements to determine the origin of fine-grained sediment at the Bermuda Rise during key climate transitions.

2. METHODS

2.1 Study Sites and Field Sampling

Table 1 lists the names and geographic locations of study sites (see Figure 6). Marine particulate samples were filtered through 293 mm Gelman A/E filters and immediately stored at -20°C to -40°C until extraction. Water samples were collected simultaneously with particulate samples. Sediment samples were taken from box cores (Sargasso Sea) or multicores (Emerald Basin) and stored in plastic bags at -20°C until extraction.

Table 1 Locations, sampling dates, and depths of samples analyzed in this study. n/a: not available

Location (sample type)		Date sampled	Water depth (m)	Sediment depth (cm)
Sargasso Sea (particulate)	31°50'N, 63°30'W	June 2000	0	
Sargasso Sea (sediment)	31°50'N, 63°30'W	June 2000	n/a	0-2
Bermuda Rise (sediment)	33°41.6'N, 57°36.7'W	July 1998	4420	0-10
Gulf of Maine (particulate)	43°15'N, 68°17'W	May 2001	0	
Emerald Basin (sediment)	45°53'N, 62°48'W	July 1998	250	0-3

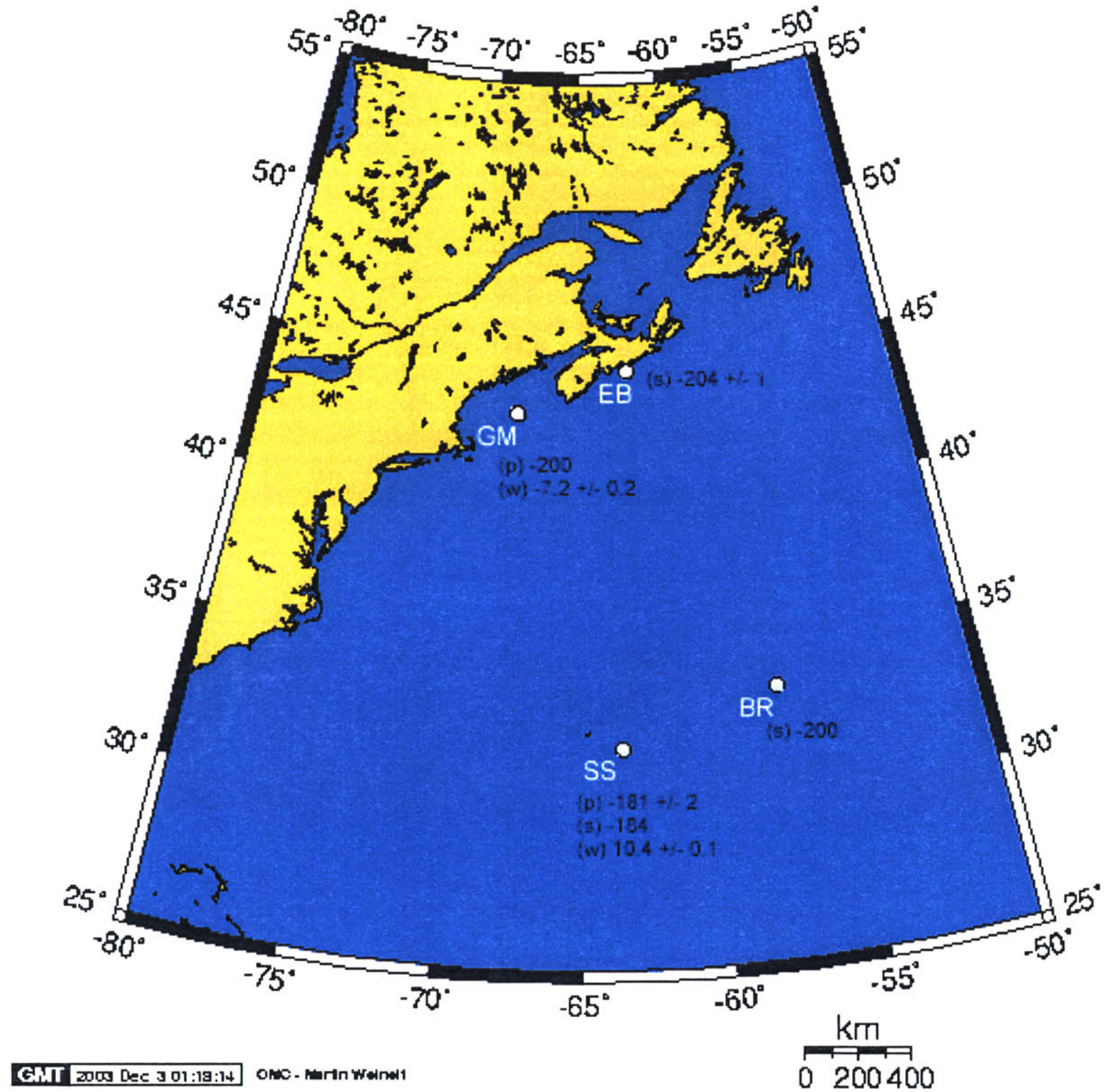
EB
(s) -204 +/- 1
GM
(p) -200
(w) -7.2 +/- 0.2
BR
(s) -200
SS
(p) -181 +/- 2
(s) -184
(w) 10.4 +/- 0.1
km
0 200 400
GMT 2003 Dec 3 01:18:14
OMC - Martin Weinelt

Figure 6.

2.2 Algal Cultures

Emiliania huxleyi strain CCMP374 was obtained from the Center for Culture of Marine Phytoplankton (CCMP), Bigelow Laboratory, Maine. The coccolithophorids, originally collected from the Gulf of Maine (42.5°N, 69°W) in 1989, were batch cultured at 18°C under a 14 hr light: 10 hr dark cycle under cool-white fluorescent lighting with a scalar irradiance of 150-250 $\mu E\ m^{-2}\ s^{-1}$ during the light cycle; light levels were measured with a QSL-100 (Biospherical Instruments) light meter. The cultures were grown at five deuterium enrichments spanning ~500‰ (Table 2) in 2 L of f/2 nutrient medium (Guillard, 1975). The f/2 medium was prepared from sterile filtered and autoclaved seawater from Vineyard Sound, MA, which has a salinity of 31.5-32.0 psu; nutrients, trace metals, vitamins, and D_2O were sterile filtered prior to addition to the sterile seawater. Media were acclimated over an 8 hr period at 18°C before inoculating the cultures at cell densities of 1-3 x 10^3 cells mL^{-1} using stocks growing in their logarithmic phases. Cultures were harvested 10-12 days after inoculation, when cell densities reached 3-5 x 10^5 cells mL^{-1}. Samples were collected by filtration through pre-combusted (450°C, > 8 hr) 47 mm Whatman GF/F filters, and immediately stored at -20°C to -40°C until extraction.

2.3 Lipid Extraction and Fractionation

Our alkenone purification procedure was adapted from Xu et al. (2001) and should be applicable to all or most alkenone-containing samples. Unless otherwise noted, all glassware was cleaned with Extran 300 concentrate and rinsed with tap water (3x), distilled water (3x), and solvent washed [methanol (3x), dichloromethane (3x), hexanes (3x)]. Pasteur pipets, glass vials, glass fiber filters, sand, Na_2SO_4, aluminum foil, and silica gel (Fisher, 100-200 mesh) were combusted at 450°C for >8 hr. Cotton was soxhlet extracted in DCM/hexane. Silver nitrate-coated silica gel (Aldrich, 10% wt:wt on 200+ mesh) was activated at 110°C overnight. After activation, silica gels were stored in 70°C drying oven.

Filters and sediments were freeze-dried (Virtis Benchtop 6.6) prior to extraction. Dried filters were cut into 1 cm strips and loaded into a stainless steel cell with 6 g Na_2SO_4, while dried sediment was loaded into a stainless steel cell with an equivalent quantity of Na_2SO_4. Samples were extracted with a Dionex ASE-200 pressurized fluid extractor using 100% DCM with three

5 min extraction cycles at 150°C and 1500 psi, and after extraction, the solvent was evaporated on a Zymark Turbovap LV (40°C). Dried total lipid extracts (TLE) (Figure 7a) (typically containing 0.5 - 20 μg alkenones) were redissolved in methanolic KOH (6% KOH in 4:1 MeOH/H_2O), sealed under N_2, and hydrolyzed at 80°C 1.5-2 hr. Extracts were then poured into a 250 mL separatory funnel containing 30 mL water and the alkenones were partitioned (3x) into 20 mL hexane. The combined hexane fractions were then back extracted (1x) with water, and applied to a Na_2SO_4 drying column. The column was rinsed (3x) with hexane, adding the rinses to the combined hexane fractions, and the solvent was evaporated under N_2. The dried extracts were then redissolved in hexane and applied to a glass 6 mL Supelco SPE tube containing 0.5 g activated 100-200 mesh silica gel in hexane. The sample was eluted with 10 mL hexane (F1 - hydrocarbons), 16 mL 1:1 DCM:hexane (F2 - alkenones), and 10 mL MeOH (F3 - pigments). Branched and cyclic molecules were then removed from the alkenone-containing fraction via the formation of urea clathrates. F2 was dissolved in 2:1 hexane/DCM and urea-adducted (3x) using methanolic urea (40 mg urea/ mL MeOH). Next, polyunsaturated ketones were separated by argentation column chromatography in a 5 3/4" pipet containing 4 cm silver nitrate- coated silica gel. The column was wet with and the sample applied using DCM, then eluted using 16 mL DCM (F1), 4 mL ethyl ether (F2 - alkenones), and 4 mL MeOH (F3). In the final silica column purification, a 5 3/4" pipet containing 4 cm 100-200 mesh silica gel was wet with and the sample applied using hexane, then eluted using 4 mL hexane (F1), 6 mL DCM (F2 - alkenones), and 4 mL MeOH. Prior to gas chromatographic analyses, dried TLE were dissolved in toluene and silylated with bis(trimethylsilyl)trifluoroacetamide (BSTFA) at 60°C for 1 hour. The purified fractions contained a distribution of C_{37}-C_{39} alkenones and most of the chromatographic baseline that interferes with both accuracy and precision in hydrogen isotopic measurements was removed (Figure 7b). Comparing the concentration of $C_{37:2-4}$ alkenones in the purified fraction to the concentration of $C_{37:2-4}$ in the TLE, we calculated a recovery of approximately 30% in both culture and marine samples. The loss of product is likely a result of the wet chemical techniques and numerous physical transfers utilized during the purification process.

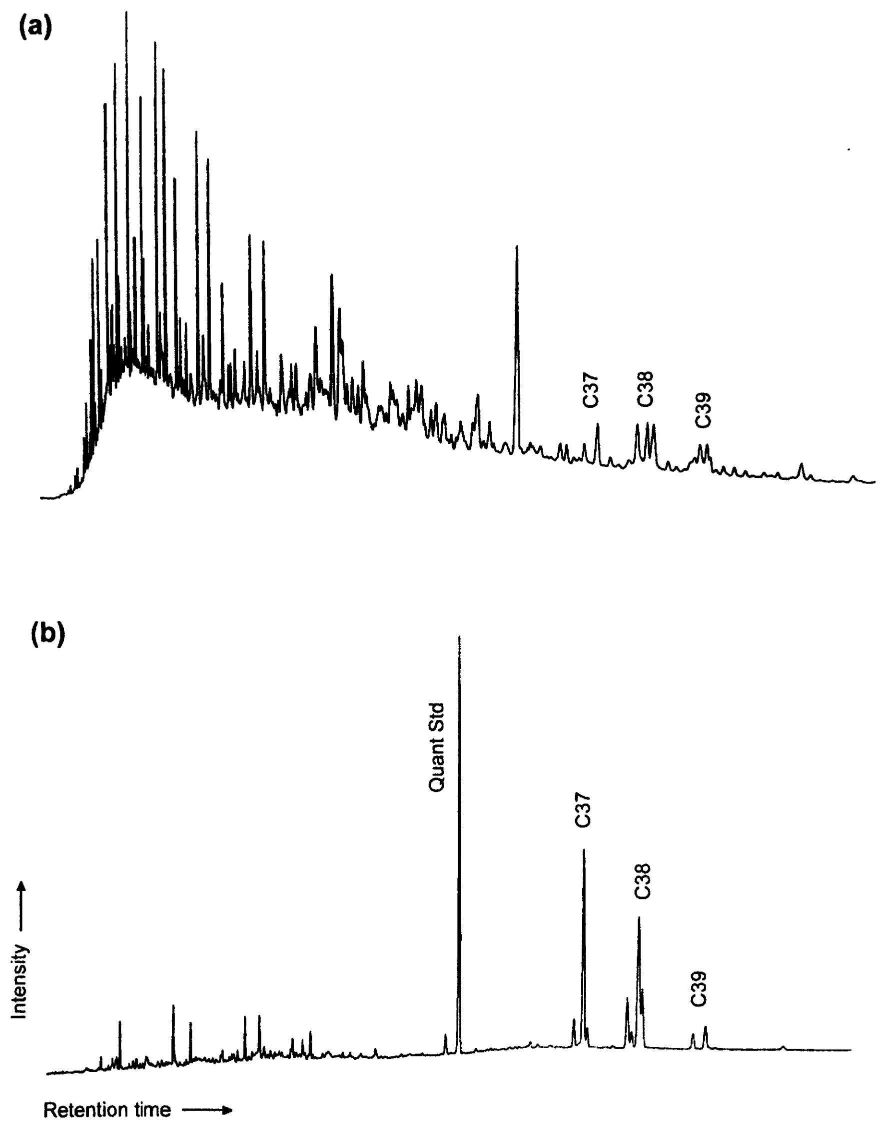

(a)
C37
C38
C39
(b)
Quant Std
C37
C38
C39
Intensity
Retention time

Figure 7.

2.4 Instrumentation

2.4.1 Gas Chromatography and Gas Chromatography - Mass Spectrometry

To identify and quantify alkenones, GC analyses were performed using Hewlett Packard 6890 Series II gas chromatographs connected to either a flame ionization detector or Agilent 5973 Mass Selective Detector. Both GC were equipped with a Hewlett Packard 7683 autoinjector, a pressure-temperature vaporization (PTV) inlet and a 60 m Chrompac CP Sil 5 capillary column (Varian). The columns were 0.32 mm i.d. with a 0.25 μm phase and a constant 1.6 mL/min flow of helium carrier gas. Both instruments used ChemStation (Agilent) acquisition software. The PTV temperature program was 60°C for 0.85 min, 60-320°C at 720°C/min, hold for 2.35 min, then 320-450°C at 720°C/min, followed by a 5 min isothermal step. The oven temperature program was 110°C for 2 min, 110-270°C at 40°C/min, 270-320°C at 2°C/min, followed by an 18 min isothermal step.

2.4.2 Isotope Ratio Monitoring Gas Chromatography Mass Spectrometry (irmGCMS)

Unless otherwise noted, hydrogen isotopic measurements were obtained at the MIT Earth, Atmospheric and Planetary Sciences Organic and Isotope Geochemistry Laboratory (OIGL). The facility consists of a Trace GC with a splitless PTV inlet coupled via GC Combustion III graphitization furnace to a DELTA^{plus} XP stable isotope ratio mass spectrometer (ThermoFinnigan, Bremen, Germany). All irmGCMS work used a 30 m capillary column with a 0.32 mm i.d. and 25 μm DB-5 phase. The PTV program was 100-325°C at 13°C/s followed by a 60 min isothermal step. The oven temperature program was 100°C for 1 min, 100-150°C at 20°C/min, 150-315°C at 10°C/min, followed by a 40 min isothermal step. A schematic of the system can be found in Figure 8. Using helium carrier gas, the effluent from the GC is fed into a graphite-lined alumina tube held at 1400°C, at which temperature organic compounds are quantitatively pyrolyzed to graphite, H_2, and CO (Burgoyne and Hayes, 1998). An open split transmits 200 uL/min of the resulting gas stream to the mass spectrometer. Data was collected and analyzed using IsoDat NT 2.0 (Thermo Electron) acquisition software.

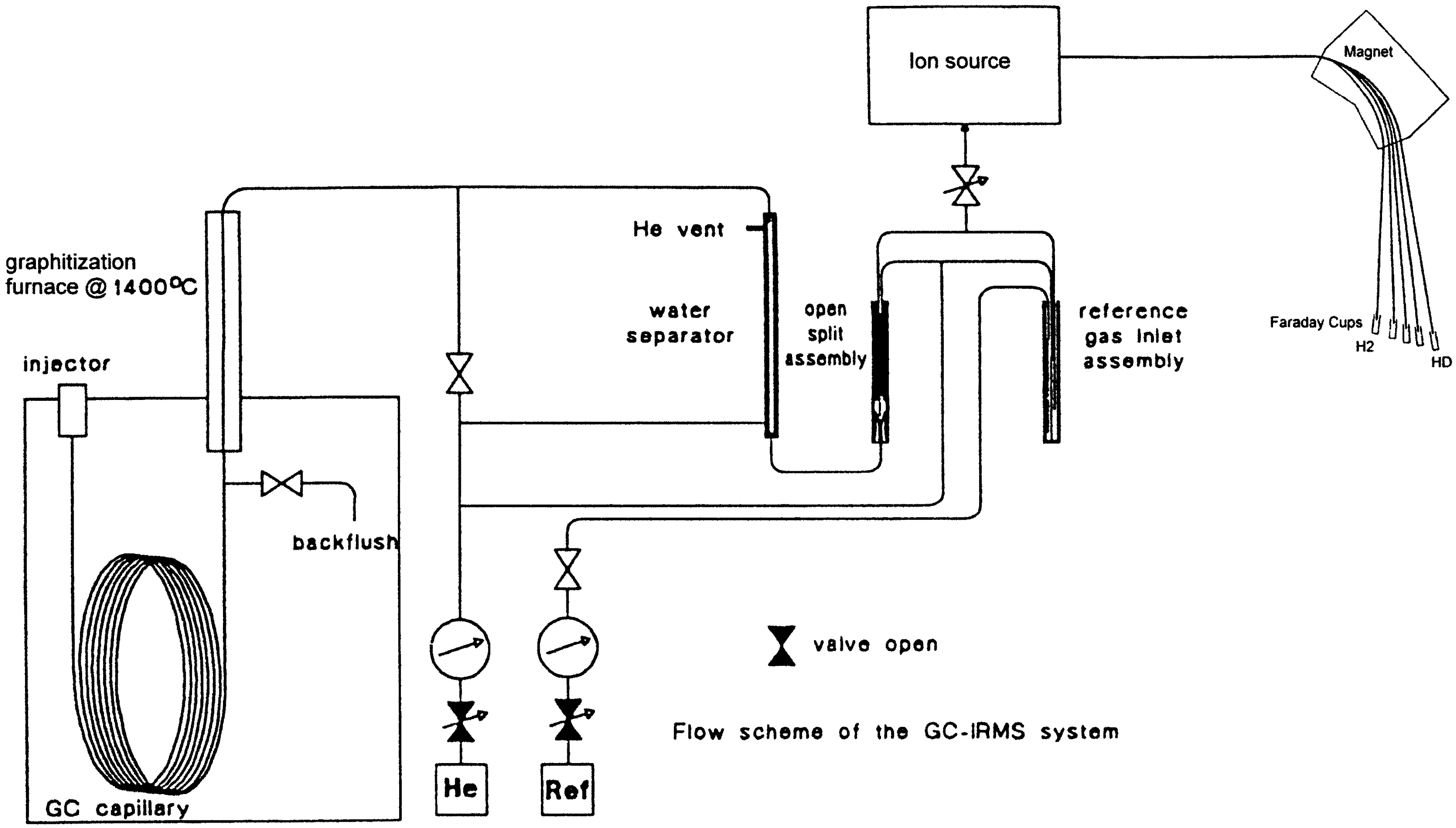
Ion source
Magnet
He vent
graphitization
furnace @ 1400°C
water
separator
open
split
assembly
reference
gas inlet
assembly
Faraday Cups
H2
HD
injector
backflush
valve open
Flow scheme of the GC-IRMS system
He
Ref
GC capillary

Figure 8.

Raw mass-3 currents are corrected for contributions from H_3^+ using an H_3^+ factor that is determined daily. Interference in measurements of HD^+ can occur because H_3^+ is formed in the ion source, and generally, the higher the hydrogen concentration in the ion source, the greater amount of H_3^+ formed there. A linearity correction is performed by measuring different H_2 concentrations in the ion source (i.e. different peak heights) and for each peak, a background correction is performed and the ratio of (area mass-3):(area mass-2) is calculated and a regression line is established covering all peaks.

Analytical results are reported as parts per thousand difference in the D/H ratio as compared to a standard reference material:

$$\delta D = \{ [(D/H)_x - (D/H)_s] / (D/H)_s \} \times 10^3$$

where x refers to the unknown sample and s refers to the standard, Vienna Standard Mean Ocean Water (VSMOW) distributed by the International Atomic Energy Agency.

Alkenone δD values were determined by reference to coinjected *n*-alkane standards obtained from Biogeochemical Laboratories, Indiana University, Bloomington, IN, USA. A mixture of 15 homologous *n*-alkanes (C_{16} - C_{30}; alkane mix "B") spanning a six-fold range in concentration and varying in δD over 210‰, and a C_{44} *n*-alkane were coinjected with each sample; two of the alkanes were used as reference peaks and the remaining provided tests of analytical accuracy and allowed normalization of δD values to the VSMOW scale (Figure 9). Because deuterium is in such low abundance in natural materials, 500-1000 ng compound were injected on-column per δD measurement. Intensities (peak areas) of 60-100 Vs typically gave the most reproducible results.

3. RESULTS

3.1 Estimates of Uncertainty

The accuracy and precision of D/H analyses of lipids is influenced by a number of factors, including variations in the H_3^+ factor and chromatographic challenges related to closely eluting compounds. For all alkenones, chromatographic resolution required reporting a pooled

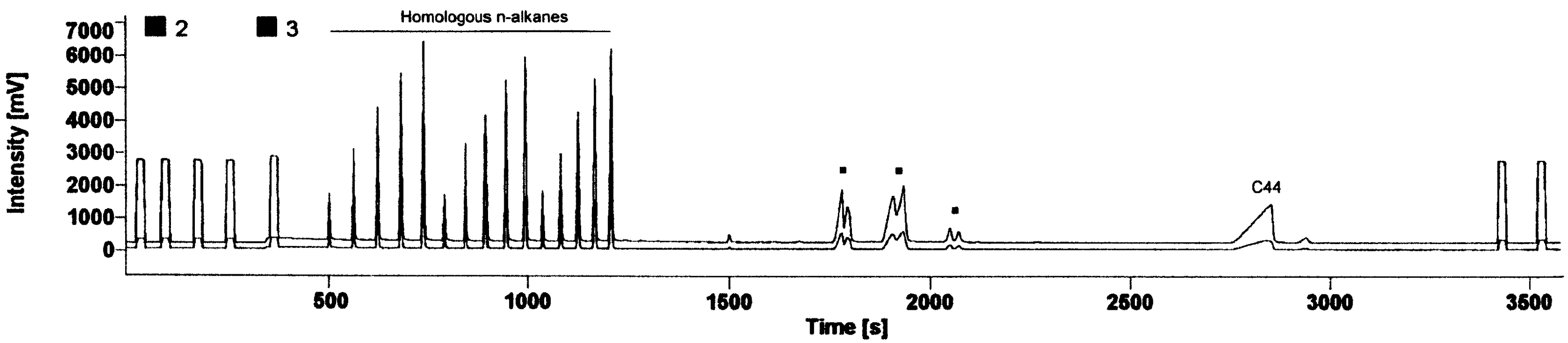

Intensity [mV]
7000
6000
5000
4000
3000
2000
1000
0
2
3
Homologous n-alkanes
C44
500
1000
1500
2000
2500
3000
3500
Time [s]

Figure 9.

isotopic value for all compounds of a given chain length (i.e. $C_{37\cdot2}$, $C_{37\ 3}$, $C_{37.4}$ reported as a pooled "$C_{37\ 2\text{-}4}$"). It is likely that differences between unsaturations of a given chain length are small, given the relatively few exchangeable hydrogens. Results from both $C_{37\cdot2\text{-}4}$ and $C_{38\cdot2\text{-}4}$ alkenones are listed in tables, and in most cases the results of each chain length were very similar, varying by < 1 to 13‰, with a median difference of -4‰ for $C_{38\ 2\text{-}4}$. We therefore propose that δD values from the $C_{38\cdot2\text{-}4}$ alkenones be used to confirm the δD value of the $C_{37\ 2\text{-}4}$ alkenones if sufficient material is unavailable to perform duplicate isotope analyses. C_{39} alkenones were also detected in the samples, but concentrations were too low for reliable isotopic measurements.

The precision of replicate analyses of a single sample was 2.9‰ (n = 34). This combines uncertainties associated with ion-current-ratio measurements, short-term variations in the pyrolysis procedure, and comparisons between sample and standard peaks in the same chromatogram. To evaluate accuracy, Sessions et al. (1999) used root mean square (RMS) error for hydrogen-isotopic analyses of a mixture of well-resolved *n*-alkanes of known isotopic composition. This represents the RMS difference between the analytical result and the known isotopic composition, and is therefore a measure of both accuracy and precision. Regression of δD by irmGCMS on δD by offline analyses of these standards provided a normalization line analogous to that used in batchwise analyses (Coplen, 1988). The RMS error of analyses of hydrocarbon standards was 5.8‰ (n = 16). This combines the noise sources listed above with all other factors, long- and short- term, affecting the placement of the samples on the δ_{VSMOW} hydrogen-isotopic scale. We can be 95% confident that the accurate value of δD_{VSMOW} for the compounds analyzed is within 2 RMS errors of the value reported.

3.2 Hydrogen Isotope Ratios in Alkenones

3.2.1 Emiliania huxleyi cultures

Hydrogen isotopic compositions of alkenones from cultures of *E. huxleyi* are summarized in Figure 10 and Table 2. Given the equation

$$\delta_P = \alpha\delta_R + 1000(\alpha - 1)$$

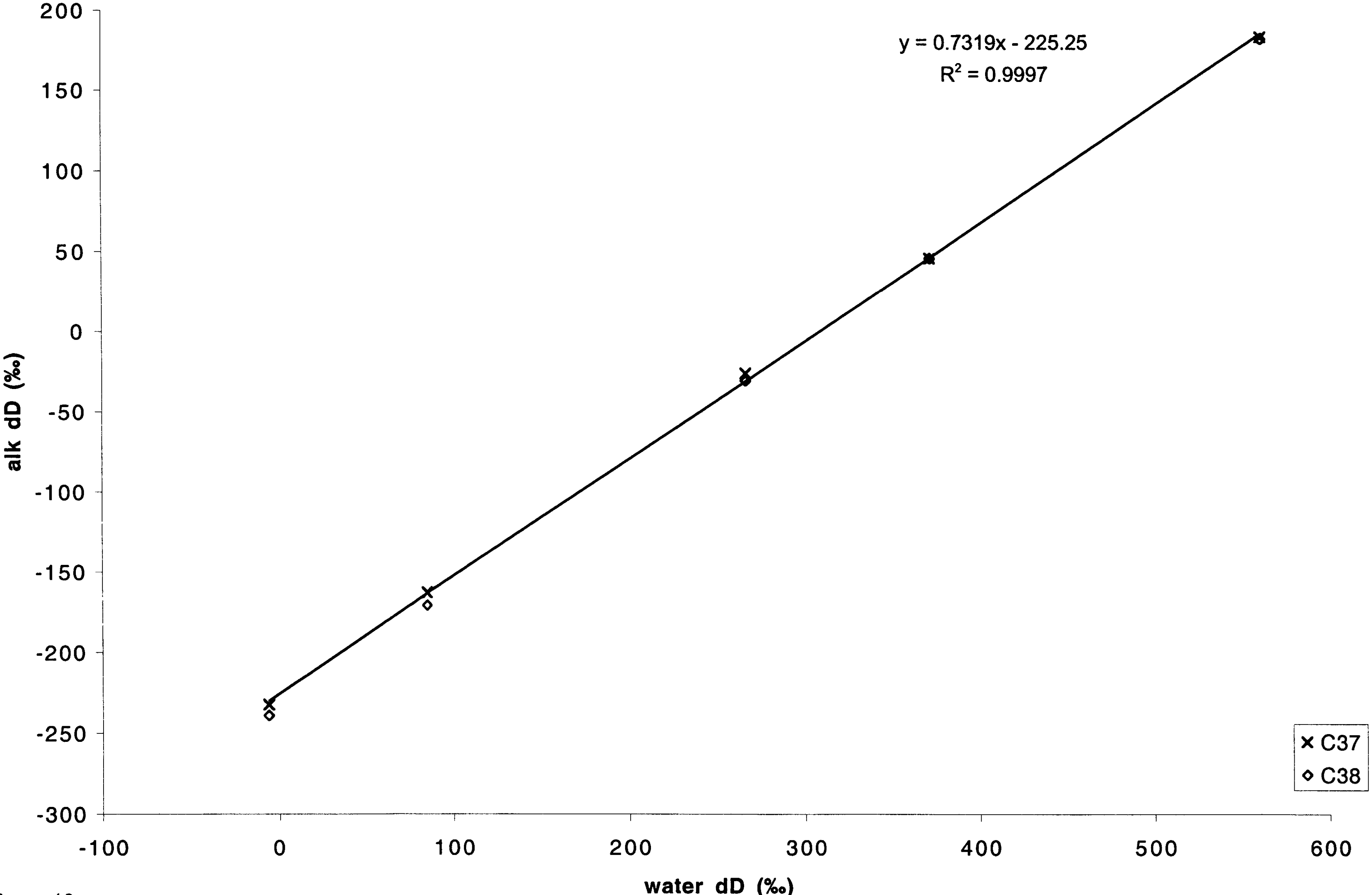
y = 0.7319x - 225.25
R² = 0.9997
alk dD (‰)
200
150
100
50
0
-50
-100
-150
-200
-250
-300
-100
0
100
200
300
400
500
600
water dD (‰)
C37
C38

Figure 10.

where δ_P is the δ associated with the products (alkenones), α is the fractionation factor, and δ_R is the δ associated with the reactants, the apparent fractionation factor associated with $C_{37\,2\text{-}4}$ alkenone biosynthesis is 0.767 with a corresponding ε ($\equiv 1000(\alpha - 1)$) of -233‰.

Table 2. Deuterium enrichments and hydrogen isotopic compositions of culture materials Water isotopic measurements were made at Stable Isotope Laboratory, Dartmouth College, Hanover, NH, and have an estimated standard deviation of 1‰. Over the 10-12 days of inoculation, water δD varied by less than 2‰. Pooled standard deviation (PSD) = $\sqrt{[(1/K)*(\Sigma S_i^2)]}$ where K is the number of groupings and S is the standard deviation of each grouping.

water δD ([D_2O] (% v/v))	alkenone δD $C_{37\,2\text{-}4}$	$\sigma_{37\,2\text{-}4}$	$\varepsilon_{37\,2\text{-}4}$	$\alpha_{37\,2\text{-}4}$	$C_{38\,2\text{-}4}$	$\sigma_{38\,2\text{-}4}$	$\varepsilon_{38\,2\text{-}4}$	$\alpha_{38\,2\text{-}4}$	n =
-6 (0)	-232	6	-227	0 773	-239	3	-234	0 766	4
85 (1E-5)	-163	1	-228	0.771	-170	1	-236	0.764	5
266 (4E-5)	-25	5	-230	0.770	-30	4	-234	0.766	4
372 (6E-5)	46	3	-236	0 764	46	2	-236	0.764	4
561 (8E-5)	183	3	-241	0.759	182	3	-242	0.758	4
PSD		4				3			

3.2.2 Marine Biomarkers

Hydrogen isotopic compositions of alkenones from marine particulate and sediment samples, as well as water samples are summarized in Figure 11 and Table 3. The range of surface water δD in the north Atlantic is mirrored by alkenone δD of suspended particles; the amplitude of ΔδD between the Sargasso Sea and the Gulf of Maine is similar for both water (17‰) and alkenones (22‰). The mean ε between $C_{37\cdot2\text{-}4}$ and surface waters in the marine samples was -193 ± 3‰ (n = 9). This isotopic depletion of alkenones in the field was 40‰ less depleted than the *E. huxleyi* cultures, -233 ± 6‰ (n = 5). Operating under the assumption that our field results are more likely to be representative of wild populations of coccolithophorids than those obtained from batch cultures we later apply the isotopic fractionation of -193‰ observed in field samples to infer the δD value of water in which the algae grew.

The D/H of particulate alkenones was very similar to the δD value of core-top sediments from each region (Figure 11). In the Sargasso Sea, the particulate alkenones had a mean δD value of -181 ± 2‰ (n = 13), while the core-top sediment had a δD value of -184‰ (n = 1). Particulate alkenones from the Gulf of Maine had a δD value of -200‰ (n = 1), while alkenones in core-top sediments from the Emerald Basin had a δD value of -204 ± 1‰ (n = 3). Further, on a time scale of days, alkenone δD values in the Sargasso Sea particles varied little, averaging

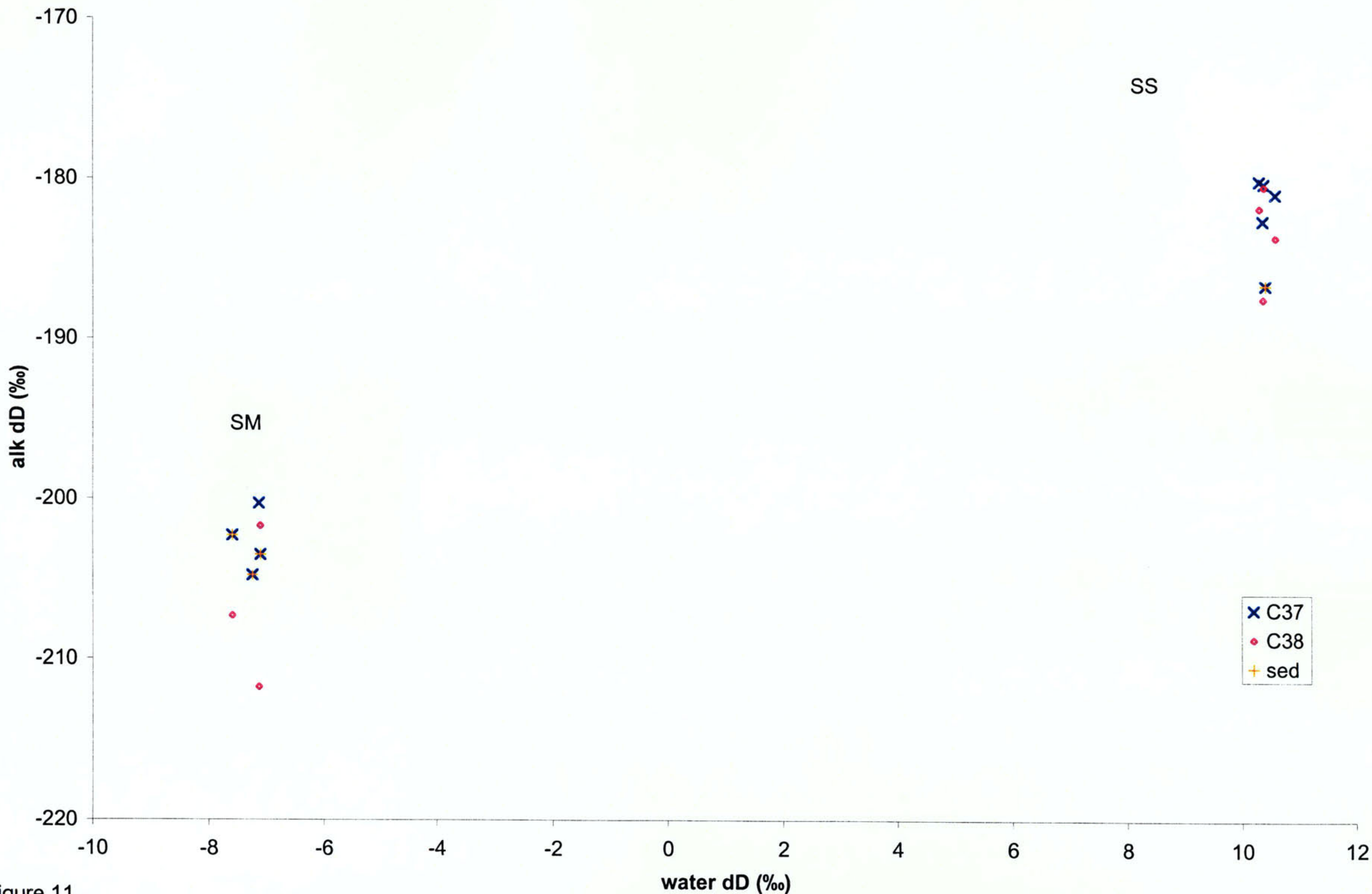

-170
-180
-190
-200
-210
-220
alk dD (‰)
SS
SM
C37
C38
sed
-10
-8
-6
-4
-2
0
2
4
6
8
10
12
water dD (‰)

Figure 11.

-181 ± 2‰ (n = 13) with a range of -180 to -182‰. Although the particulate samples represent a snapshot in time whereas the sediments average over tens to thousands of years, the difference in δD values for each was within our measurement error. In addition, alkenone δD shows distinctive deuterium signatures of northern (more depleted) and southern (less depleted) source waters, but does not vary greatly within those regions. The mean δD values of all alkenones (particulate and sedimentary) analyzed in the Sargasso Sea and Scotian Margin regions, respectively, were -182 ± 3‰ (n = 14) and -203 ± 2‰ (n = 4).

Table 3. Isotopic compositions of marine particulate (part) and sediment (sed) samples from Sargasso Sea (SS), Gulf of Maine (GM), and Emerald Basin (EB), and water samples collected simultaneously with particulate samples. The pooled standard deviation (PSD) of the 13 injections of Sargasso Sea particulate samples is reported beneath those entries. Hydrogen isotopic measurements of water were made at Stable Isotope Laboratory, Dartmouth College, Hanover, NH, and have an estimated standard deviation of 1‰. Oxygen isotopic measurements were made at Laboratory for Geochemical Oceanography, Harvard University and have an estimated standard deviation of 0.03‰.

	alkenone δD							water	
sample type	$C_{37\,2\text{-}4}$	$\sigma_{37\,2\text{-}4}$	$\varepsilon_{37\,2\text{-}4}$	$C_{38\,2\text{-}4}$	$\sigma_{38\,2\text{-}4}$	$\varepsilon_{38\,2\text{-}4}$	n =	δD	$\delta^{18}O$
SS part	-182	1	-191	-187	3	-182	3	10.35	1.12
SS part	-181	3	-189	-184	1	-178	3	10.57	1.18
SS part	-180	1	-189	-180	2	-174	3	10.37	1.09
SS part	-180	1	-188	-182	2	-176	4	10.29	1.13
SS part	-159*	7*					4		
SS part	-161*	8*					4		
PSD		2			2				
SS sed (0-2 cm)	-184**		-195					10.40	
GM part	-200		-195	-212		-206		-7.11	-1.26
EB sed (0-3 cm)									
0.5 cm	-204**		-198						
0.5 cm	-202		-196	-202		-196			
2.5 cm	-205		-199	-207		-201			

* measured Isotope Organic Geochemistry Laboratory, Brown University, Mar 2001. δD values were not used in final statistical analyses because raw isotope values were based on comparison to reference gas pulses rather than coinjected standards, as was used for evaluation and normalization of the rest of the data. On both OIGL and WHOI irmGCMS instruments, reference hydrogen tanks have been observed to "drift" throughout the sample runs by 7-10‰ (S. Sylva, pers. comm.)
** measured in J. Hayes laboratory, WHOI, Dec 2002

Data from box core sub-core OCE326-BC9J are summarized in Figure 12 and Table 4. Keigwin (1996) and Ohkouchi et al. (2002) previously examined this same box core to investigate late Holocene and glacial-interglacial climate change. Weight-percent $CaCO_3$ decreases from a maximum at 4.5 cm to a pronounced minimum centered on 1.5 cm. We follow the work of Keigwin (1996), in attributing the carbonate minimum and preceding maximum to the climate events loosely known as the Little Ice Age (LIA) and Medieval Warm Period (MWP), respectively. δD values increase from a low prior to and including the MWP, to a high

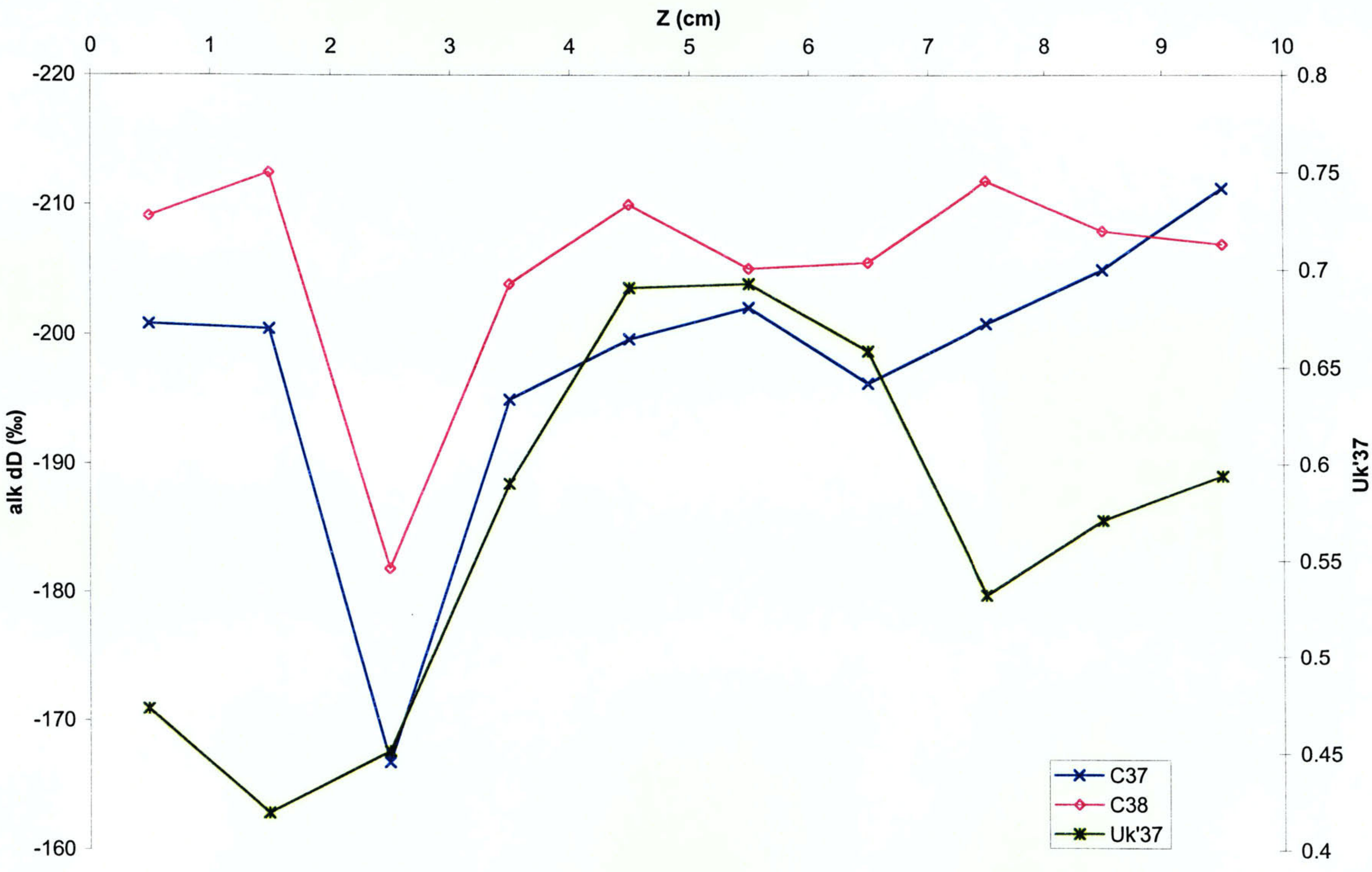

Figure 12.

at 2.5 cm, then return to more depleted values at the core-top. $U^{k'}_{37}$ values indicate a SST maximum centered at 5 cm followed by a minimum at 1.5 cm.

Table 4 Alkenone δD, U^{k}_{37} ratio, and carbonate content for Bermuda Rise core OCE326-BC9J (this study) as well as alkenone ^{14}C age and U^{k}_{37} ratio from Ohkouchi et al. (2002). n.a.. not analyzed

sediment	alkenone δD				(Ohkouchi et al., 2002)	
depth (cm)	$C_{37\,2\text{-}4}$	$C_{38\,2\text{-}4}$	$U^{k'}_{37}$	% $CaCO_3$	^{14}C age	U^{k}_{37}
0.5	-201	-209	0.4728	24.9	6230	0.577
1.5	-200	-213	0.4185	17.8	5060	0.524
2.5	-167	-182	0.4507	20.4	7810	0.495
3.5	-195	-204	0.5895	23.9	n.a.	0.601
4.5	-199	-210	0.6907	45.5	5780	0.675
5.5	-202	-205	0.6927	31.6		
6.5	-197	-206	0.6582	32.4		
7.5	-201	-212	0.5319	31.9		
8.5	n.a.	n.a.	0.5707	32.7		
9.5	-212	-207	0.5940	30.1	3100	0.848

4. DISCUSSION

4.1 Alkenone δD in Deuterium-Enriched Cultures

At the time of harvest, a small but non-negligible fraction of isotopically-depleted alkenones in the cultures likely remained from the seed culture which was maintained in seawater with a δD value of -7‰. This contribution of depleted inoculum could increase the apparent fractionation of the culture. However, based on the maximum percentage of inoculant in the harvested culture (0.8%), the effect is likely small, corresponding to < 2‰ difference in the most enriched culture.

4.2 Alkenone δD in Suspended Particles

Because we cultured a single strain of *E. huxleyi,* the difference between culture and field results may reflect real differences in the hydrogen isotopic fractionation associated with alkenone biosynthesis in different strains or species of coccolithophorids. Discrepancies between culture and field results are common in alkenone unsaturation calibrations (e.g. González et al., 2001; Herbert, 2001) and are generally ascribed to different responses of cells in culture vs. natural field environments. It is not immediately clear whether batch or continuous growth models better represent natural conditions or whether the sinking flux of alkenones and alkenoates in the ocean comes from populations in exponential, late logarithmic, or stationary growth state. Rather different biochemical responses can be obtained from the same strain of alkenone-producing algae cultured in batch or continuous modes (Popp et al., 1998) and from the phase of growth from which alkenones are harvested (Conte et al., 1998; Epstein et al., 1998).

E. huxleyi is the dominant coccolithophorid in many of the world's oceans (Berge, 1962; Okada and Honjo, 1973, 1975; Okada and McIntyre, 1977, 1979; Nishida, 1986), is believed to be the main producer of alkenones in the open ocean (Volkman et al., 1980; Marlowe et al., 1984a,b, 1990), and constitutes between 40-87% of the coccoliths in surface sediments from the greater part of the North Atlantic Ocean (Geitzenauer et al., 1977). However, the species exists as genetically different strains, and it is now apparent that these can have different lipid compositions that respond differently to temperature change (e.g. Sikes and Volkman, 1993; Conte and Eglinton, 1993; Conte et al., 1994). Variability in intracellular alkenone composition has also been noted to have a physiological as well as genetic component (Conte et al., 1998; Epstein et al., 1998), and algal cells are well known to undergo complex modifications of their intracellular and membrane compositions (e.g., Shuter 1979 and references therein) in response to growth regulating environmental factors such as nutrient availability, light, and trace micronutrient concentrations (e.g., Sunda and Huntsman, 1995).

The presence of a freshwater lense could also affect the δD of our particulate samples. GEOSECS sampling through the water column in the North Atlantic (Ostlund et al., 1987) showed a salinity decrease of approximately 1.5 psu was accompanied by a decrease in δD of approximately 7‰ over 5000 m water depth. Therefore, some portion of the 22‰ ΔδD of the northern and southern regions could have resulted from salinity differences but the similarity between multiple samples taken in the same geographic regions, as well as the similarity between particulate and sediment coretops indicate that it is not likely to be solely a salinity signal.

4.3 Provenance of Alkenones at the Bermuda Rise from δD

We can use the alkenone δD and alkenone-derived SST values to infer where alkenones in Bermuda Rise sediment were synthesized. Taken together, the δD and $U^{k'}_{37}$ values indicate that alkenones, and by extrapolation, fine-grained sediment, were being transported to the Bermuda Rise from a region of relative warm SST and deuterium-depleted waters during the MWP, cold and less depleted waters just prior to the LIA, and cold and depleted waters during the LIA. Ohkouchi et al. (2002) suggested that the Bermuda Rise is influenced by more than two sources that are similar but not identical, and concluded that the observed range of alkenone ^{14}C ages indicated highly variable processes delivering fine material to the Bermuda Rise. These variations could result from changes in provenance or modes of transport, and while ^{14}C work can indicate the variability of the processes affecting the fine fraction signal, the δD signature could allow a greater understanding of the regions from which the material is derived.

At the Bermuda Rise, it is likely that carbonate flux was relatively constant and the flux of terrigenous sediment delivered by deep currents increased during the LIA (Keigwin, 1996), just as it did during earlier carbonate minima in the Holocene and during glaciation (Bacon and Rosholt, 1982; Suman and Bacon, 1989). This terrigenous sediment most likely was resuspended from the Scotian Rise during abyssal storms (Hollister and McCave, 1994) or eroded from the northeast scarp of the Bermuda Rise (Laine et al., 1994).

In summer, a strong SST gradient is observed directly south of the Scotian Margin (Figure 13). If high-latitude alkenones record a SST signal weighted toward summer averages, when most blooms occur (Iglesias-Rodriguez et al., 2002), subtle shifts in source across the SST gradient could result in $U^{k'}_{37}$ signal variability of 0.45-0.85 while being sourced from a region of nearly constant surface water δD (Figure 3).

The δD enrichment at 2.5 cm, which we believe to be robust because it is observed in both $C_{37\,2\text{-}4}$ and $C_{38.2\text{-}4}$, corresponds to an anomalously old sample in Ohkouchi et al. (2002). The alkenones in this depth interval could indicate an eastward shift in source toward 45°N, 40°W, giving rise to a cold but relatively D-enriched alkenone signal. This particular area lies between the Labrador Sea and Sohm Abyssal Plain, and it is recognized that material from the Labrador Sea finds its way to the Sohm Abyssal Plain in turbidity currents (Laine and Hollister, 1981). Emerging from the LIA, the source of alkenones to the Bermuda Rise may have shifted westward again, back to the Scotian Margin and the vicinity of strong SST gradient, producing the cold and deuterium-depleted alkenone signal we observe (Figure 12).

Assuming that the hydrogen isotopic distribution in the North Atlantic did not change significantly over this time scale, mass balance calculations using Sargasso Sea and Scotian

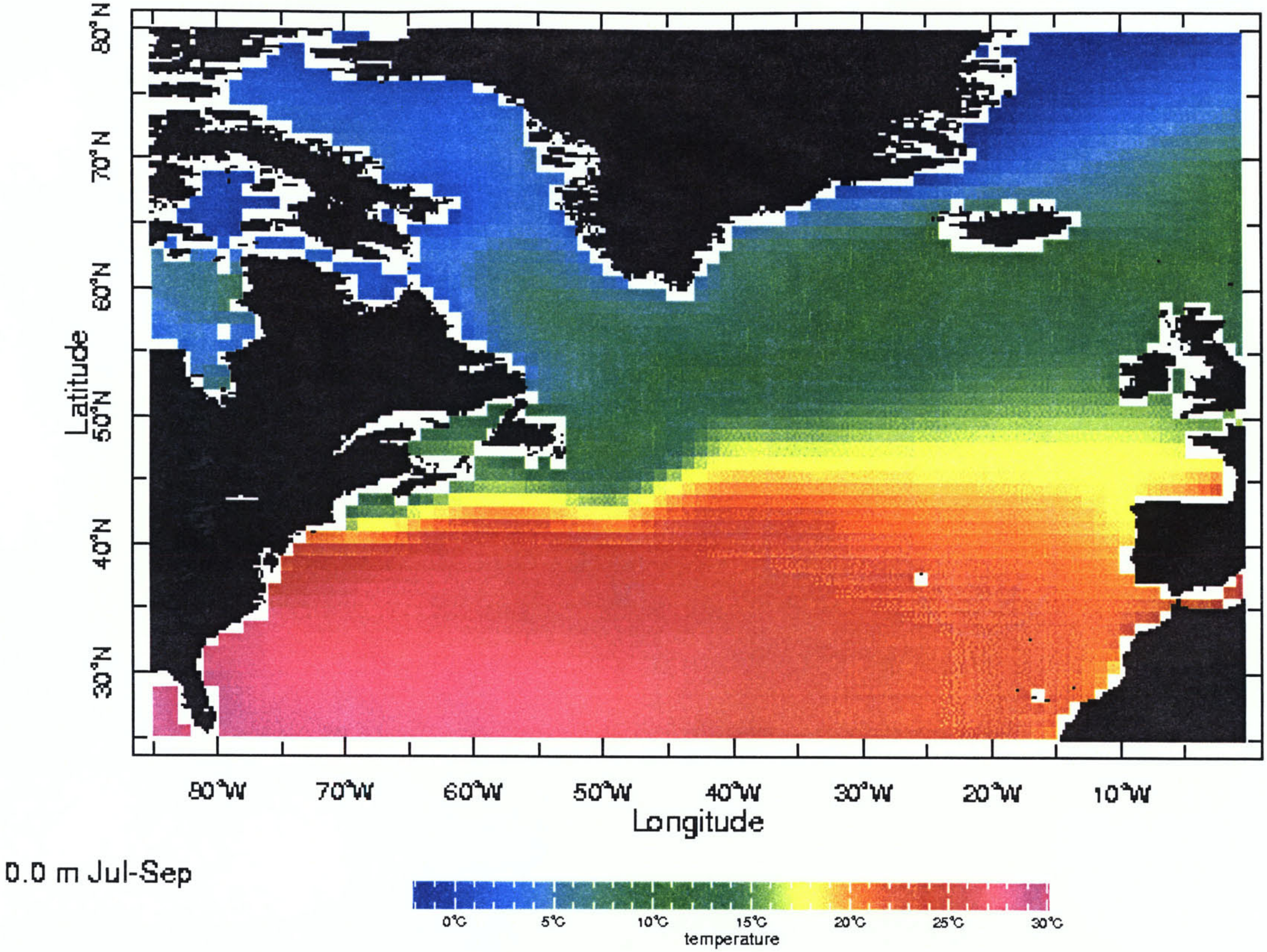

80°N
70°N
60°N
50°N
40°N
30°N
Latitude
80°W
70°W
60°W
50°W
40°W
30°W
20°W
10°W
Longitude
0.0 m Jul-Sep
0°C
5°C
10°C
15°C
20°C
25°C
30°C
temperature

Figure 13

Margin δD as end members (-182‰ and -203‰, respectively, with standard deviations less than 3‰) indicate that at most depths in the core, greater than 60% of the alkenones were produced in isotopically-depleted waters. If northern latitude alkenones are produced predominantly in the summer in the presence of the strong SST gradient, the use of "average" $U^{k'}_{37}$ values in mass balance calculations may not provide an accurate picture of the alkenone mixing taking place in the region. Therefore, using the Prahl et al. (1988) $U^{k'}_{37}$ calibration, we calculated the contributions of non-local material at the Bermuda Rise. End-members were chosen to represent the summer (Jul-Sep) SST range at the Scotian Margin (12-24°C), late winter/early spring bloom at the Bermuda Rise (19°C; OCL, 1998; Conte et al., 2001), and the Bermuda Rise summer average (26.5°C; OCL, 1998; Table 5 and Figure 14). These results are comparable to Ohkouchi et al. (2002) who used average Laurentian Fan and Bermuda Rise $U^{k'}_{37}$ of 0.4 and 0.8, respectively, to estimate 0-75% of the material at the Bermuda Rise was transported from elsewhere. When compared to the δD mass balance calculations, it is evident that linear mixing does not explain the patterns in alkenone, and by extension, fine-fraction delivery to the Bermuda Rise.

Table 5 Fraction non-local material in Bermuda Rise core OCE326-BC9J using mass balance calculations of both $U^{k'}_{37}$ and δD with Scotian Margin (SM) and Bermuda Rise (BR) end-members. SST ranges (combinations denoted by SM SST/BR SST) encompass Jul-Sep SST gradient (12-24°C) near SM and both average SST during coccolithophorid seasonal bloom (19°C) and average Jul-Sep SST (26.5°C) at BR. Ohkouchi et al. performed similar mass balance calculations using mean annual Laurentian Fan and BR $U^{k'}_{37}$ of 0.4 and 0.8, respectively. All $U^{k'}_{37}$ to SST conversions used Prahl et al. (1988) calibration. δD end-members were average δD of SM (-203‰) and SS (-182‰).

sediment depth (cm)	Fraction non-local (SM SST/BR SST) 12/19	24/19	12/26.5	24/26.5	Ohkouchi 10.6/22.4	δD
0.5	0.475	0.248	1	0.546	0.558	0 944
1.5	0.596	0.312	1	0.610	0.691	0.889
2.5	0.524	0.274	1	0.572	0.764	0
3.5	0 214	0.112	0.784	0.410	0.498	0 611
4 5	0	0	0.558	0.292	0.313	0 833
5.5	0	0	0.553	0.289		1
6 5	0.060	0 031	0.630	0.330		0.722
7.5	0.343	0.179	0.913	0.477		0.944
8.5	0 256	0.134	0.826	0.432		
9.5	0.204	0.106	0.774	0.405	0	1

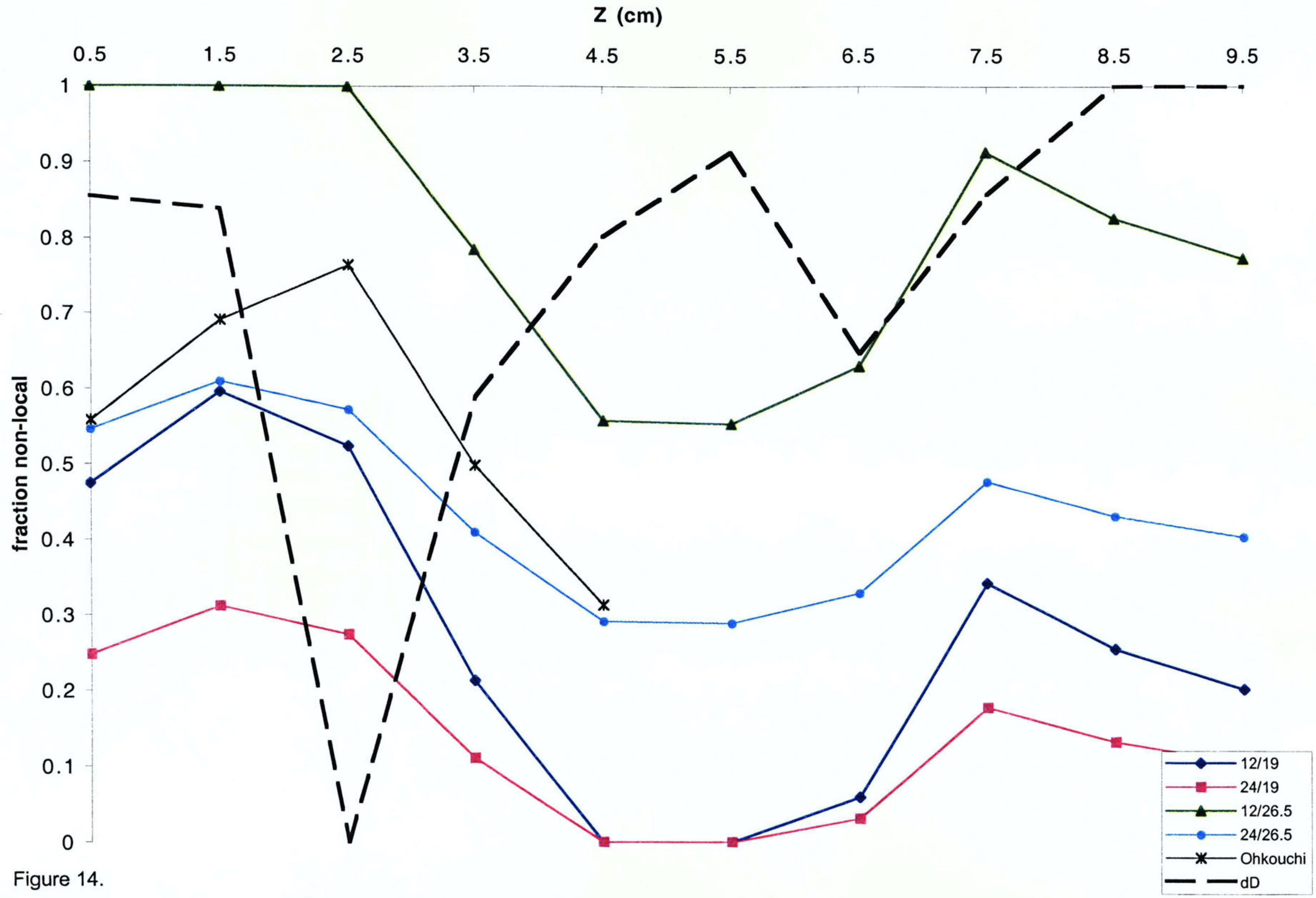
Z (cm)
0.5
1.5
2.5
3.5
4.5
5.5
6.5
7.5
8.5
9.5
1
0.9
0.8
0.7
0.6
0.5
0.4
0.3
0.2
0.1
0
fraction non-local
12/19
24/19
12/26.5
24/26.5
Ohkouchi
dD

Figure 14.

5. CONCLUSIONS

The new data presented here show that variations in alkenone D/H reflect, at least in part, differences in growth water D/H and the use of hydrogen isotopes in alkenones shows promise as a new paleoclimate proxy for sediment provenance in the marine environment. While additional culture work is necessary to understand the nuances of hydrogen isotopic fractionation during alkenone biosynthesis, the highly reproducible isotopic depletions of -193 ± 3‰ (n = 9) in field samples and -233 ± 6‰ (n = 5) in batch cultures, relative to water, supports the use of alkenones as hydrogen isotopic surrogates for surface water. The average $\Delta\delta D$ between the Sargasso Sea and Scotian Margin was similar for water (17‰) and alkenone (22‰) samples and hydrogen isotopic variations in alkenones have been used to predict surface ocean δD to within 6‰. In addition, particulate alkenone δD was within measurement error of the average sediment alkenone δD in each region. Alkenone δD varied in the top 10 cm of Bermuda Rise core OCE326-BC9J by 45‰, suggesting a change in phytoplankton detritus source region during the climate periods loosely known as the Medieval Warm Period and Little Ice Age. Further, alkenone δD analyses are a complementary approach to the alkenone ^{14}C age determination pioneered by Ohkouchi et al. (2002) because while ^{14}C work can indicate the variability of the processes affecting the fine fraction signal, the alkenone δD signature allows a more direct analysis of the geographic regions from which the fine material is derived. In addition, alkenone δD requires less material than alkenone ^{14}C and allows analyses of climate events beyond the ^{14}C timescale. Using mass balance calculations to determine the fraction of non-local material at the Bermuda Rise, discrepancies between alkenone-derived δD and $U^{k'}_{37}$ indicate that linear mixing does not explain the patterns in alkenone, and by extension, fine-fraction delivery to the Bermuda Rise.

This approach could be used in other regions of high sediment accumulation with a pronounced gradient in surface water δD. In the Argentine Basin, for example, strong bottom currents transport material from the south into this region (Ledbetter, 1986), and recent work by Benthein and Müller (2000) shows that modern bottom sediments in the basin record temperatures that are 2-6°C cooler than the sea surface. Additionally, improved chromatographic resolution and separation of individual alkenones would allow the analysis and comparison of specific compounds, rather than pooling isotopic results from suites of same-chain-length compounds, allowing greater flexibility in regions that may not have as strong a δD gradient as the North Atlantic.

It was demonstrated by Sauer et al. (2001) that lipid δD can be used to derive surface water hydrogen isotope stratigraphies in places where oxygen isotope stratigraphies are not possible. Alkenone δD also shows promise for these types of climate studies in regions such as in the Southern Ocean, deep Pacific, or many lakes where carbonate microfossils are either not produced or not preserved.

Another worthwhile extension of this work would be an examination of inter-species differences in hydrogen isotopic expression. Although *E. huxleyi* is the predominant Haptophyte in most open ocean coccolithophorid blooms, better understanding of the δD changes associated with species variations would allow this method to be applied to other oceanic regions and during time periods before the evolution of *E. huxleyi*. However, care must be taken in the assumption of constant surface ocean isotopic distribution for times in the more distant past.

The measurement of stable hydrogen isotopic ratios in alkenones shows promise as a new paleoclimate proxy and in conjunction with alkenone-derived SST determination and other approaches such as Ohkouchi et al. (2002) alkenone ^{14}C age determination, is a powerful approach that can provide targeted paleoenvironment information.

ACKNOWLEDGEMENTS

NSF Graduate Research Fellowship to A.C.E.; D. Repeta, D. Kulis, S. Haley, S. Sylva, E. Roosen, Woods Hole Oceanographic Institution; C. Colonero, Z. Zheng, MIT; A. Faiia, Dartmouth College; A. Schimmelmann, P. Sauer, Indiana University; A. Sessions, Caltech; D. Schrag, Harvard University; Y. Huang, Brown University; E. Head, Bedford Institute of Oceanography

References for Chapter 2

Adkins J. F., Boyle E. A., Keigwin L., and Cortijo E. (1997) Variability of the North Atlantic thermohaline circulation during the last interglacial period. *Nature* **390,** 154-156.

Bacon M. P. and Rosholt J. N. (1982) Accumulation rates of Th-230, Pa-231, and some transition metals on the Bermuda Rise. *Geochim. Cosmochim. Acta* **46,** 651-666.

Benthien A. and Müller P. J. (2000) Anomalously low alkenone temperatures caused by lateral particle and sediment transport in the Malvinas Current region, western Argentine Basin. *Deep-Sea Res. I* **47,** 2369-2393.

Berge G. (1962) Discoloration of the sea due to a *Coccolithus huxleyi* "bloom". *Sarsia* **6,** 27-40.

Buchardt B. and Fritz P. (1980) Environmental isotopes as environmental and climatological indicators. In *Handbook of Environmental Isotope Geochemistry,* Vol. 1 (ed. P. Fritz and J. C. Fontes) pp. 473-504. Elsevier, Amsterdam.

Burgoyne T. W. and Hayes J. M. (1998) Quantitative production of H_2 by pyrolysis of gas chromatographic effluents. *Anal. Chem.* **70,** 5136-5141.

Charles C. D., Lynch-Stieglitz J., Ninnemann U. S. and Fairbanks R. G. (1996) Climate connections between the hemisphere revealed by deep sea sediment core / ice core correlations. *Earth Planet. Sci. Lett.* **142,** 19-27.

Conte M. H. and Eglinton G. (1993) Alkenone and alkenoate distributions within the euphotic zone of the eastern North Atlantic: correlation with production temperature. *Deep-Sea Res.* **40,** 1935-1961.

Conte M. H., Thompson A., Lesley D. and Harris R. P. (1998) Genetic and physiological influences on the alkenone/alkenoate versus growth temperature relationship in *Emiliania huxleyi* and *Gephyrocapsa oceanica. Geochim. Cosmochim. Acta* **62,** 51-68.

Conte M. H., Volkman J. K. and Eglinton G. (1994) Lipid biomarkers of the Haptophyta. In *The Haptophyte Algae* (ed. J. C. Green and B. S. C. Leadbeater) pp. 351-77. Clarendon Press.

Conte M. H., Weber J. C., King L. L. and Wakeham S. (2001) The alkenone temperature signal in western North Atlantic surface waters. *Geochim. Cosmochim. Acta* **65,** 4275-4287.

Coplen T. B. (1988) Normalization of oxygen and hydrogen isotope data. *Chemical Geology* **72,** 293-297.

Craig H. (1961) Isotopic variations in meteoric waters. *Science* **133,** 1702-1703.

Dansgaard W. (1964) Stable isotopes in precipitation. *Tellus* **16,** 436-468.

Draut A. E., Raymo M. E., McManus J. F. and Oppo D. W. (2003) Climate stability during the Pliocene warm period. *Paleoceanography* **18,** 1078-1089.

Epstein B. L., D'Hondt S., Quinn J. G., Zhang J. and Hargraves P. E. (1998) An effect of dissolved nutrient concentrations on alkenone-based temperature estimates. *Paleoceanography* **13,** 122-126.

Epstein S., Yapp C. J. and Hall J. H. (1976) The determination of the D/H ratios of non-exchangeable hydrogen in cellulose extracted from aquatic and land plants. *Earth and Planet. Sci. Lett.* **30,** 241-251.

Friedman I., Carrara P. and Gleason J. (1988) Isotopic evidence of Holocene climatic change in the San Juan Mountains, Colorado. *Quat. Res.* **30,** 350-353.

Geitzenauer K. R., Roche M. B. and McIntyre A. (1977) Coccolith biogeography from North Atlantic and Pacific surface sediments. In *Oceanic Micropaleontology* (ed. A. T. S. Ramsey) pp. 973-1008. Academic Press.

González E. L., Riebesell U., Hayes J. M. and Laws E. A. (2001) Effects of biosynthesis and physiology on relative abundances and isotopic compositions of alkenones. *Geochem. Geophys. Geosyst.* **2,** 2000GC000052.

Guillard R. R. L. (1975) Culture of phytoplankton for feeding marine invertebrates. In *Culture of Marine Invertebrate Animals* (ed. W. L. Smith and M. H. Chanley) pp. 29-60. Plenum Press.

Herbert T. D. (2001) Review of alkenone calibrations (culture, water column, and sediments). *Geochem. Geophys. Geosyst.* **2,** 2000GC000055.

Hoering T. C. (1984) Thermal reactions of kerogen with added water, heavy water, and pure organic substances. *Org. Geochem.* **5,** 267-278.

Hollister C. D. and McCave I. N. (1994) Sedimentation under deep-sea storms. *Nature* **309,** 220-225.

Iglesias-Rodriguez M. D., Brown C. W., Doney S. C., Kleypas J., Kolber D., Kolber Z., Hayes P. K. and Falkowski P. G. (2002) Representing key phytoplankton functional groups in ocean carbon cycle models: coccolithophorids. *Global Biogeochem. Cycles* **16,** 1100-1119.

Keigwin L. D. (1996) The Little Ice Age and Medieval Warm Period in the Sargasso Sea. *Science* **274,** 1504-1508.

Keigwin L. D. and Jones G. A. (1989) Glacial-Holocene stratigraphy, chronology, and paleoceanographic observations on some North Atlantic sediment drifts. *Deep-Sea Res.* **36,** 845-867.

Keigwin L. D. and Pickart R. S. (1999) Slope water current over the Laurentian Fan on interannual to millennial time scales. *Science* **286,** 520-523.

Koepp M. (1978) D/H isotope exchange reaction between petroleum and water: a contributory determinant for D/H-isotope ratios in crude oils? In *Short papers of the 4th International Conference, Geochronology, Cosmochronology, Isotope Geology. USGS Open File Report* (ed. R.E. Zartman) pp. 78-701. US Geological Survey.

Laine E. P. and Hollister C. D. (1981) Geological effects of the Gulf Stream system on the Northern Bermuda Rise. *Mar. Geol.* **39,** 277-310.

Laine E. P., Gardner W. D., Richardson M. J. and Kominz M. (1994) Abyssal currents and advection of resuspended sediment along the northeastern Bermuda Rise. *Mar. Geol.* **119,** 159-171.

Ledbetter M. T. (1986) Bottom-current pathways in the Argentine Basin revealed by mean silt particle-size. *Nature* **321,** 423-425.

Lehman S. J., Sachs J. P., Crotwell A. M., Keigwin L. D. and Boyle E. A. (2002) Relation of subtropical Atlantic temperature, high-latitude ice rafting, deep water formation, and European climate 130,000-60,000 years ago. *Quat. Sci. Rev.* **21,** 1917-1924.

Luo Y-H., Sternberg L. dS. L., Suda S., Kumazawa S. and Mitsui A. (1991) Extremely low D/H ratios of photoproduced hydrogen by cyanobacteria. *Plant Cell Phys.* **32,** 897-900.

Marlowe I. T., Brassell S. C., Eglinton G. and Green J.C. (1984a) Long chain unsaturated ketones and esters in living algae and marine sediments. *Org. Geochem.* **6,** 135-141.

Marlowe I. T., Green J. C., Neal A. C., Brassell S. C., Eglinton G. and Course P. A. (1984b) Long chain (n-C_{37}-C_{39}) alkenones in the Prymnesiophyceae. Distribution of alkenones and other lipids and their taxonomic significance. *Br. Phycol. J.* **19,** 203-216.

Marlowe I. T., Brassell S. C., Eglinton G. and Green J.C. (1990) Long-chain alkenones and alkyl alkenoates and the fossil coccolith record of marine sediments. *Chem. Geol.* **88,** 349-375.

Martin G. J., Zhang B. L., Naulet N. and Martin M. L. (1986) Deuterium transfer in the bioconversion of glucose to ethanol studied by specific isotope labeling at the natural abundance level. *J. Amer. Chem. Soc.* **108,** 5116-5122.

McCave I. N. (2002) A Poisoned Chalice? *Science* **298,** 1186-1187.

McManus J. F., Bond G. C., Broecker W. S., Johnsen S., Labeyrie L. and Higgins S. (1994) High-resolution climate records from the North Atlantic during the last interglacial. *Nature* **371,** 326-329.

Miller R. F. (1991) Chitin paleoecology. *Biochem. Sys. Ecol.* **19,** 401-411.

Miller R. F., Fritz P. and Morgan A. V. (1988) Climatic implications of D/H ratios in beetle chitin. *Palaeogeog. Palaeoclim. Palaeoecol.* **66,** 277-288.

Nishida S. (1986) Nannoplankton flora in the Southern Ocean, with special reference to siliceous varieties. *Mem. NIPR Spec. Issue* **40,** 56-68.

Ocean Climate Laboratory, *World Ocean Atlas, 1998.* National Oceanographic Data Center, Silver Spring, MD.

Ohkouchi N., Eglinton T. I., Keigwin L. D. and Hayes J. M. (2002). Spatial and temporal offsets between proxy records in a sediment drift. *Science* **298,** 1224-1227.

Okada H. and Honjo S. (1973) The distribution of oceanic coccolithophorids in the Pacific. *Deep-Sea Res.* **20,** 355-374.

Okada H. and Honjo S. (1975) Distribution of coccolithophores in marginal seas along the western Pacific Ocean and in the Red Sea. *Mar. Biol.* **31,** 271-285.

Okada H. and McIntyre A. (1977) Modern coccolithophores of the Pacific and North Atlantic Ocean. *Micropaleontology* **23,** 1-55.

Okada H. and McIntyre A. (1979) Seasonal distribution of modern coccolithophores in the western North Atlantic Ocean. *Mar. Biol.* **54,** 319-328.

Ostlund H. G., Craig H., Broecker W. S. and Spenser D. (1987) GEOSECS Atlantic, Pacific and Indian Ocean expeditions: Shorebased Data and Graphics, vol. 7. *Tech. rep.* Nat. Sci. Found. Washington D.C.

Popp B. N., Kenig F., Wakeham S. G. and Bidigare R. R. (1998) Does growth rate affect ketone unsaturation and intracellular carbon isotopic variability in *Emiliania huxleyi*? *Paleoceanography* **13,** 35-41.

Prahl F. G., Meuhlhausen L. A. and Zahnle D. L. (1988) Further evaluation of long-chain alkenones as indicators of paleoceanographic conditions. *Geochim. Cosmochim. Acta* **52,** 2303-2310.

Prahl F. G. and Wakeham S. G. (1987) Calibration of unsaturation patterns in long-chain ketone compositions for palaeotemperature assessment. *Nature* **330,** 367-369.

Raymo M. E., Ganley K., Carter S., Oppo D. W. and McManus J. (1998) Millennial-scale climate instability during the early Pleistocene epoch. *Nature* **392,** 699-702.

Rechka J. A. and Maxwell J.R. (1988) Characterization of alkenone temperature indicators in sediments and organisms. *Org. Geochem.* **13,** 727-734.

Rozanski K., Araguas-Araguas L. and Gonfiantini R. (1992) Relation between long-term trends of oxygen-18 isotope composition of precipitation and climate. *Science* **258,** 981-985.

Sachs J. P., Anderson R. F. and Lehman S. J. (2001) Glacial surface temperatures of the Southeast Atlantic Ocean. *Science* **293,** 2077-2079.

Sachs J. P. and Lehman S. J. (1999) Subtropical North Atlantic temperatures 60,000 to 30,000 years ago. *Science* **286,** 756-759.

Sauer P. E., Eglinton T. I., Hayes J. M., Schimmelmann A. and Sessions A. L. (2001) Compound-specific D/H rations of lipid biomarkers from sediments as a proxy for environmental and climatic conditions. *Geochim. Cosmochim. Acta* **65,** 213-222.

Schimmelmann A. and DeNiro M. J. (1986) Stable isotopic studies on chitin III. The $^{18}O/^{16}O$ and D/H ratios in arthropod chitin. *Geochim. Cosmochim. Acta* **50,** 1485-1496.

Schimmelmann A., DeNiro M. J., Poulicek M., Voss-Foucart M.-F., Goffinet G. and Jeauniaux C. (1986) Isotopic composition of chitin from arthropods recovered in archaeological contexts as palaeoenvironmental indicators. *J. Archaeol. Sci.* **13,** 553-566.

Schmidt G. A., Bigg G. R. and Rohling E. J. (1999) Global seawater oxygen-18 database. http://www.giss.nasa.gov/data/o18data/

Schoell M. (1984) Stable isotopes in petroleum research. *Adv. Petrol. Geochem.* **1,** 215-245.

Sessions A. L., Burgoyne T. W., Shimmelmann A. and Hayes J. M. (1999) Fractionation of hydrogen isotopes in lipid biosynthesis. *Org. Geochem.* **30,** 1193-2000.

Shuter B. (1979) A model of physiological adaptation in unicellular algae. *J. Theor. Biol.* **78,** 519-552.

Sikes E. L. and Volkman J. K. (1993) Calibration of alkenone unsaturation ratios ($U^{K'}_{37}$) for paleotemperature estimation in cold polar waters. *Geochim. Cosmochim. Acta* **57,** 1883-1889.

Smith J. W., Rigby D., Schmidt P. W. and Clark D. A. (1983) D/H ratios of coals and the paleoaltitude of their deposition. *Nature* **302,** 322-323.

Smith B. N. and Epstein S. (1970) Biogeochemistry of the stable isotopes of hydrogen and carbon in salt marsh biota. *Plant Phys.* **46,** 738-742.

Sternberg L. dS. L. (1988) D/H ratios of environmental water recorded by D/H ratios of plant lipids. *Nature* **333,** 59-61.

Suman D. O. and Bacon M. P. (1989) Variations in Holocene sedimentation in the North American Basin determined from ^{230}Th measurements. *Deep Sea Res.* **36,** 869-878.

Sunda W. G. and Huntsman S. A. (1995) Iron uptake and growth limitation in oceanic and coastal phytoplankton. *Mar. Chem.* **50,** 189-206.

Volkman J. K., Barrett S. M., Blackburn S. I. and Sikes E. L. (1995) Alkenones in *Gephyrocapsa oceanica*: implications for studies of paleoclimate. *Geochim. Cosmochim. Acta* **59,** 513-520.

Volkman J. K., Eglinton G., Corner E. D. S. and Sargent J. R. (1980) Novel unsaturated straight-chain methyl and ethyl ketones in marine sediments and a coccolithophore *Emiliania huxleyi*. In *Advances in Organic Geochemistry, 1979* (ed. A. G. Douglas and J. R. Maxwell) pp. 219-227. Pergamon, Tarrytown, N.Y.

Werstiuk N. H. and Ju C. (1989) Protium-deuterium exchange of benzo-substituted heterocycles in neutral D_2O at elevated temperatures. *Can. J. Chem.* **67,** 812-815.

Xu L., Reddy C. M., Farrington J. W., Frysinger G. S., Gaines R. B., Johnson C. G., Nelson R. K. and Eglinton T. I. (2001) Identification of a novel alkenone in Black Sea sediments. *Org. Geochem.* **32,** 633-645.

Yapp C. J. and Epstein S. (1982) Climatic significance of the hydrogen isotope ratios in tree cellulose. *Nature* **297,** 636-639.

Chapter 3: Conclusions

3.1 General Conclusions

Temporal records in cores from lakes and ocean sediments, in coral reefs, and in polar ice encode information on natural variations of the climate system. Geochemical proxies that reflect past environmental conditions are employed to understand large-scale shifts in climate, and compound-specific hydrogen isotopic analyses represent one of the newest proxies to be utilized. Rapidly deposited ocean sediments provide the best archive for studying rapid climate changes through geologic time, but a major potential concern for utilizing a multiple proxy approach at drift sites arises from the possibility that the climate proxies associated with the fine fraction of sediment may be chronologically and spatially decoupled from those associated with the coarse fraction.

The research presented in this thesis was undertaken to better understand the source of the fine fraction of sediment that is deposited at the Bermuda Rise. The new data presented here show that variations in alkenone D/H reflect, at least in part, differences in growth water D/H and the use of hydrogen isotopes in alkenones shows promise as a new paleoclimate proxy for sediment provenance in the marine environment. The following conclusions can be made:

1) Alkenone δD can be measured in marine particles and sediments by isotope ratio monitoring gas chromatography mass spectrometry with a precision greater than 6‰. The procedure relies on multiple wet chemical and chromatographic purifications and requires ~500-1000 ng alkenones injected on-column per sample.
2) While additional work is necessary to understand the nuances of hydrogen isotopic fractionation during alkenone biosynthesis, the isotopic depletions of -233 ± 6‰ (n = 5) in batch cultures of *Emiliania huxleyi* and -193 ± 3‰ (n = 9) in the particulate marine samples, relative to water, supports the use of alkenone D/H as hydrogen isotopic surrogates for surface water.
3) The average ΔδD between the Sargasso Sea and Scotian Margin was similar for water (17‰) and alkenone (22‰) samples, and particulate alkenone δD was within measurement error of the average sediment alkenone δD in each region.

4) δD was measured in both $C_{37:2-4}$ and $C_{38\ 2-4}$ alkenones, and in most cases the results of each chain length were very similar, varying by < 1 to 13‰, with a median difference of -4‰ for $C_{38:2-4}$. We therefore propose that δD values from the $C_{38\ 2-4}$ alkenones be used to confirm the δD value of the $C_{37\ 2-4}$ alkenones. In this way, one can evaluate the accuracy of a value even if sufficient material is unavailable to perform duplicate isotope analyses.
5) Alkenone δD varied in the top 10 cm of Bermuda Rise core BC-9J by 45‰, suggesting a change in phytoplankton detritus source region during the climate periods loosely known as the Medieval Warm Period and Little Ice Age. Further, alkenone δD analyses are a complementary approach to the alkenone ^{14}C age determination pioneered by Ohkouchi et al. (2002) because while ^{14}C work can indicate the variability of the processes affecting the fine fraction signal, the alkenone δD signature allows analysis of the regions from which the fine material is derived. In addition, alkenone δD requires less material than alkenone ^{14}C and allows analyses of climate events beyond the ^{14}C timescale.
6) Using mass balance calculations to determine the fraction of non-local material at the Bermuda Rise, alkenone δD indicates that at most depths analyzed, greater than 60% of the alkenones were sourced from a region of relatively D-depleted waters. However, discrepancies between alkenone-derived δD and $U^{k'}_{37}$ indicate that linear mixing does not explain the patterns in alkenone, and by extension, fine-fraction delivery to the Bermuda Rise.

3.2 Directions for Future Research

This approach could be used in other regions of high sediment accumulation with a pronounced gradient in surface water δD. In the Argentine Basin, for example, strong bottom currents transport material from the south into this region (Ledbetter, 1986), and recent work by Benthein and Müller (2000) shows that modern bottom sediments in the basin record temperatures that are 2-6°C cooler than the sea surface. Additionally, improved chromatographic resolution and separation of individual alkenones would allow the analysis and comparison of specific compounds, rather than pooling isotopic results from suites of same-chain-length compounds, allowing greater flexibility in regions that may not have as strong a δD gradient as the North Atlantic.

It was demonstrated by Sauer et al. (2001) that lipid δD can be used to derive surface water hydrogen isotope stratigraphies in places where oxygen isotope stratigraphies are not possible. Alkenone δD also shows promise for these types of climate studies in regions such as in the Southern Ocean, deep Pacific, or many lakes where carbonate microfossils are either not produced or not preserved.

Another worthwhile extension of this work would be an examination of inter-species differences in hydrogen isotopic expression. Although *E. huxleyi* is the predominant Haptophyte in most open ocean coccolithophorid blooms, better understanding of the δD changes associated with species variations would allow this method to be applied to other oceanic regions and during time periods before the evolution of *E. huxleyi*. However, care must be taken in the assumption of constant surface ocean isotopic distribution for times in the more distant past.

The measurement of stable hydrogen isotopic ratios in alkenones shows promise as a new paleoclimate proxy and in conjunction with alkenone-derived SST determination and other approaches such as Ohkouchi et al. (2002) alkenone ^{14}C age determination, is a powerful approach that can provide targeted paleoenvironment information.

References for Chapter 3

Benthien A. and Müller P. J. (2000) Anomalously low alkenone temperatures caused by lateral particle and sediment transport in the Malvinas Current region, western Argentine Basin. *Deep-Sea Res. I* **47,** 2369-2393.

Ledbetter M. T. (1986) Bottom-current pathways in the Argentine Basin revealed by mean silt particle-size. *Nature* **321,** 423-425.

Ohkouchi N., Eglinton T. I., Keigwin L. D. and Hayes J. M. (2002). Spatial and temporal offsets between proxy records in a sediment drift. *Science* **298,** 1224-1227.

Sauer P. E., Eglinton T. I., Hayes J. M., Schimmelmann A. and Sessions A. L. (2001) Compound-specific D/H rations of lipid biomarkers from sediments as a proxy for environmental and climatic conditions. *Geochim. Cosmochim. Acta* **65,** 213-222.

Appendix: Figure Captions

Figure 1. Chemical structures of di-, tri-, and tetra- unsaturated C_{37}-C_{39} alkenones; n = 5, 6, 7 and R = CH_2CH_3 or CH_3. The double bonds are in the biologically rare trans configuration (Rechka and Maxwell, 1988). Figure from Conte et al., 1998.

Figure 2. The meteoric relationship for ^{18}O and ^{2}H in precipitation. Data are weighted average annual values for precipitation monitored at stations in the International Atomic Energy Agency global network, compiled in Rozanski et al. (1992).

Figure 3. Surface distribution of deuterium excess (top 50 m) over the globe, using the relationship $\delta D = 10.72 + 7.25\ \delta^{18}O$ ($r^2 = 0.98$) (Schmidt et al., 1999).

Figure 4. Sediment drift deposits; samples from the Bermuda Rise (northwest Atlantic) were used in this study.

Figure 5. Turbidity currents (tan) from the Laurentian fan (LF) are entrained by deep-ocean flows (blue arrows) and trapped in regions of recirculation (pale blue areas) (Schmitz and McCartney, 1993). Resuspension from the upper continental margin of Nova Scotia and the northern US feeds into the recirculating gyre and may find its way to the Bermuda Rise. North Atlantic Deep Water (NADW) (thick blue arrow). WBUC, Western Boundary Undercurrent. Figure from McCave, 2002.

Figure 6. Locations of samples analyzed in this study. Particulate samples were acquired from the Sargasso Sea (SS) and Gulf of Maine (GM), and sediments were acquired from the Sargasso Sea, Bermuda Rise (BR), and Emerald Basin (EB). Detailed site locations can be found in Table 1.

Figure 7. Representative chromatograms of (a) TLE and (b) alkenone fraction after purification.

Figure 8. Schematic overview of irmGCMS system used in MIT Organic and Isotope Geochemistry Laboratory.

Figure 9. Representative chromatogram from irmGCMS analyses. A mixture of 15 homologous *n*-alkanes (C_{16}-C_{30}) as well as nC_{44} were coinjected with each sample (alkenones marked with •). Accuracy and precision are best when the sample is closely bracketed by standards.

Figure 10. Hydrogen isotopic compositions of alkenones from *Emiliania huxleyi* cultures grown at five deuterium enrichments. The average fractionation factor, 0.767, corresponds to an isotopic fractionation of -233, and is within two RMS errors of the slope and intercept, respectively. That the slope and intercept correspond to α and ε is a characteristic of single-step isotopic fractionations.

Figure 11. Comparison of hydrogen isotopic compositions of marine particulate and sediment samples from the Sargasso Sea (SS) versus Emerald Basin and Gulf of Maine (loosely grouped

as Scotian Margin (SM) Both $C_{37:2\text{-}4}$ and $C_{38:2\text{-}4}$ δD were measured on particulate samples; only $C_{37:2\text{-}4}$ δD was measured in sediment.

Figure 12. Alkenone δD and $U^{k'}_{37}$ in first 10 cm of Bermuda Rise core OCE326-BC9J. $U^{k'}_{37} \equiv (37{:}2)/(37{:}2 + 37{:}3)$ (Prahl and Wakeham, 1987; Prahl et al., 1988).

Figure 13. Jul-Sep SST in North Atlantic (OCL, 1998).

Figure 14. Fraction non-local material in Bermuda Rise core OCE326-BC9J using mass balance calculations of both $U^{k'}_{37}$ (symboled lines) and δD (heavy dashed line) with Scotian Margin (SM) and Bermuda Rise (BR) end-members. SST ranges (combinations denoted by SM SST/BR SST) encompass Jul-Sep SST gradient (12-24°C) near SM and both average SST during coccolithophorid seasonal bloom (19°C) and average Jul-Sep SST (26.5°C) at BR. Ohkouchi et al. (2002) performed similar mass balance calculations using mean annual Laurentian Fan and BR $U^{k'}_{37}$ of 0.4 and 0.8, respectively (x). All $U^{k'}_{37}$ to SST conversions used Prahl et al. (1988) calibration. δD mass balance end-members were average δD of SM (-203‰) and BR (-182‰).